Lunar and Planetary Science XXII

Abstracts of papers submitted to the Twenty-Second Lunar and Planetary Science Conference

PRESS ABSTRACTS

NASA

National Aeronautics and
Space Administration

Lyndon B. Johnson Space Center
Houston, Texas

LPI / USRA

LUNAR AND PLANETARY INSTITUTE
UNIVERSITIES SPACE RESEARCH ASSOCIATION

PRESS ABSTRACTS

TWENTY-SECOND LUNAR AND PLANETARY SCIENCE CONFERENCE

March 18 - 22, 1991

Compiled by the
Lunar and Planetary Institute
3303 NASA Road 1
Houston Texas 77058-4399

LPI Contribution Number 758

Business Telephone Numbers of First Authors

E. Asphaug 602-621-2773

V. R. Baker 602-621-6003

T. J. Bernatowicz 314-889-6274

A. G. W. Cameron (correspondence author) 617-495-5374

A. L. Deino 415-644-1295

R. Greeley 602-965-7045

J. K. Harmon 804-878-2612

J. W. Head III 401-863-2526

P. B. James 419-537-4906

T. V. V. King 303-236-1373

R. L. Kirk 602-527-7020

R. V. Krishamurthy 818-356-6137

R. Landheim 318-257-2858

T. McDonnell 44-227-459616

D. S. McKay 713-483-5048

C. R. Neal 219-239-8328

R. S. Saunders 818-393-0877

F. J. Stadermann 49-6221-516453

K. L. Tanaka 602-527-7208

PREFACE

The Program Committee for the Twenty-second Lunar and Planetary Science Conference has chosen these contributions as having the greatest potential interest for the general public. The papers in this collection have been written for general presentation, avoiding jargon and unnecessarily complex terms. More technical abstracts will be found in *Lunar and Planetary Science XXII*.

For assistance during the conference, call the NASA Johnson Space Center News Center at 713-483-5111. Telephone numbers of the first author of each contribution will be found on page iii. Feel free to call for more information.

CONTENTS

Impact Processes in the Solar System: New Understandings through Numerical Modeling

E. Asphaug and H.J. Melosh (Lunar and Planetary Laboratory, Tucson)
E. Ryan (Planetary Science Institute, Tucson)

Imagine two rocky objects circling the sun in space, each roughly the size and mass of a large mountain range. A random component of their orbits moves them towards one another at a velocity many times faster than a supersonic jet. To what degree can we predict the outcome of such a collision?

Rudimentary energy calculations lead us to expect an almost inconceivably violent catastrophe, whose magnitude — about one billion megatons — would greatly exceed all of our thermonuclear stockpiles detonating at once. Extensive melting and vaporization would occur, along with explosive fragmentation, high-velocity ejection of debris in many directions, and an overall change in the orbits. But can we establish this in a more quantitative sense? We must strive to do so, for much of our understanding of the solar system depends on what we know about these kinds of hypervelocity impact processes.

According to our current interpretations of solar system evolution, impacts such as the one above were the basis for planetary growth, or *accretion*. Circling the new sun some 4.6 billion years ago was a cloud of gas and dust which soon condensed into small asteroid-like objects called *planetesimals*. The mechanism for this condensation is not well-understood, but it involved gas drag and collisions. The planetesimals, in turn, impacted with one another on a regular basis until their relative velocities were damped enough for them to gravitationally bind together — leading to the growth of planets. Typical impact velocities in the current asteroid belt are ~ 5 km/s; in the past they were probably a few times greater, and far more frequent. It is an open question whether the asteroids we see today are unaccreted remnants of the planetesimal swarm.

Consider the impact described above, occurring in free space. If the collisional velocity is great enough, fragments will be dispersed: from the two impactors we will get dozens or hundreds or thousands of minor objects flying out at independent trajectories.

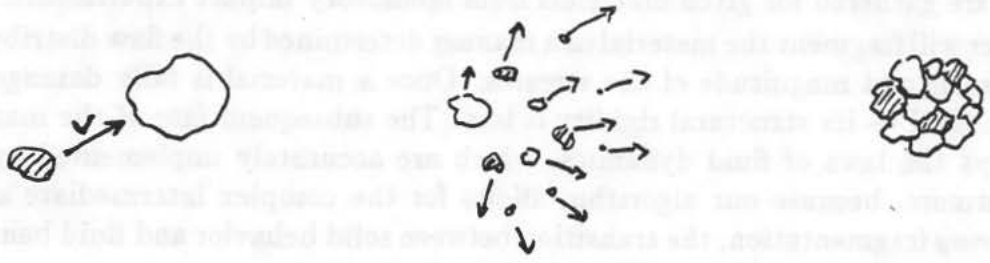

Figure 1. (a) The projectile approaching the target at velocity v. (b) The outcome for a velocity much greater than the threshold, with projectile and target fragments dispersing. (c) The outcome for a velocity lower than the threshold, with relatively large fragments gravitationally reaccreting. Intermediate outcomes are also possible.

But at some lower threshold velocity, the disruptive effect of the catastrophe will no longer exceed the mutual gravity, and the material will clump into a single object whose momentum is the sum of the two colliding parents. There will in fact be a range of such outcomes: intermediate velocities, for instance, might expel some fragments but leave a large aggregated body behind. These scenarios are illustrated in Figure 1.

These threshold velocities are clearly dependent on the masses of the impactors. (Equivalently, if we assume a typical encounter velocity of some 5 km/s, then we could talk about a threshold mass.) Tiny dust grains would have virtually no gravitational binding energy, so the threshold velocity would be low. Colliding planets (*c.f.* the "giant impact" scenario for the ejection of the Moon from the proto-Earth), on the other hand, would have to involve much greater velocities to result in dispersion. One early qualitative approach was to characterize impacts by their *Safronov number*, which is essentially the ratio of gravitational binding energy to impact energy. If the Safronov number is large, then the bodies will coalesce; if it is small, dispersion of fragments will occur. But this is hardly the level of quantitative precision we need for the sophisticated models of planetary accretion that are now possible with high-speed computers. These models, to be accurate, require specific outcomes for specific impacts. Given, say, a 100 km projectile impacting a 300 km target at 5 km/s, what will the fragment size distribution look like? What will the velocities of these fragments be? How much mass will escape from the bodies, and how much will be gravitationally re-accreted? To what degree will the material be altered by shock pressurization, melting and vaporization? What direction will the ejected fragments take?

To answer these important questions, our group has developed a *fragmentation hydrocode* to perform dynamical computations of collisional outcomes. Our impact research takes two seemingly unrelated sciences — explosive fragmentation and fluid dynamics — and draws them together into a single application. To model a solid, we input certain material parameters, such as density, elasticity, rigidity, and energies of melting and vaporization. These parameters are well-known for a variety of important materials, such as ice, iron, granite and basalt. Another important parameter is the distribution of initial flaws within the material. These flaws are the locations where fractures can initiate; each flaw has associated with it a yield stress above which it will begin to grow. Flaw distributions are gathered for given materials from laboratory impact experiments.

An impact will fragment the material in a manner determined by the flaw distribution and the timescale and magnitude of the stresses. Once a material is fully damaged, it behaves like a fluid — its structural rigidity is lost. The subsequent fate of the material therefore obeys the laws of fluid dynamics, which are accurately implemented by the code. Furthermore, because our algorithm allows for the complex intermediate states that occur *during* fragmentation, the transition between solid behavior and fluid behavior is not abrupt, but follows the impact stresses through the target.

Figure 2 shows the fragmentation sequence for a typical target — in this case, a 22 km target being hit by a small projectile to model the impact into the Martian satellite Phobos (Figure 3) that created the crater Stickney, which dominates one hemisphere. The projectile hits at the top center. The half-circle represents a small wedge of the

target, like a slice of an apple: the experiment takes place with rotational symmetry such that the left-hand straight boundary is the central axis. This sequence illustrates the propagation of the "damage pulse" through the target; undamaged material (farthest from the impact) obeys the physics of a solid, whereas fully damaged material (closest to the impact) is best described as a fluid. The material inbetween is in transition — it is undergoing rubblization by the stress waves of the impact. Free-surface interactions are evident, since without them the pulse would be hemispherical; the final frame shows the undamaged regions remaining in the target. Besides causing extensive damage, the impact accelerates the fragmented material and provides the fragments with velocities that might carry them off.

This code is the first successful, *i.e.* predictive, two-dimensional model of continuum fragmentation that we know of; we have been able to consistently reproduce the results of laboratory fragmentation experiments with high precision. Because the code is based on physical (rather than phenomenological) rules of material behavior, the sizes and velocities that characterize an impact can be varied at will, as long as the physics involved does not change. We do, for instance, incorporate gravity into our models for impactors larger than about 30 km. Our knowledge of collisional outcomes is therefore extended far beyond the range achievable in the laboratory, where $\sim$ 10 cm objects are the largest sizes, and self-gravity is totally untestable.

The collisional event that created the crater Stickney, for instance, can be modeled as easily as a meteoric dust grain hitting an icy ring particle around Saturn, or the ejection of surface material from a major asteroid such as Vesta. Along a different vein, we can simulate cratering impacts into planetary surfaces — such as the one that launched the SNC meteorites from the surface of Mars, sending them into trajectories that brought them to Earth.

In addition to enabling us to extrapolate to large sizes, we can observe the process of fragmentation at arbitrarily small *timescales*. Prior to photographic studies, "collisional outcomes" was synonymous with "fragment size distributions," since all that could be done was to gather and sieve the debris. (A fragment size distribution is a plot of the number of fragments in each size range.) Modern high-speed film analyses give far more complete results, and show the velocities and rotation rates of the fragments. But the *process* is not captured on film: the fastest film rates are still far slower than the timescale of a typical laboratory impact event, some 20 millionths of a second. (And even if we achieved million-frame-per-second film rates, how could we observe what is happening inside of a target?) The fragmentation hydrocode allows us to step through a fragmentation event in arbitrarily small timesteps, viewing the propagation of the stress wave through the target, its interaction with free surfaces, the onset of fragmentation, and the velocities of fragments accelerated by the impact.

This "numerical laboratory" should provide significant insights into the many puzzles of planetary accretion, asteroid regoliths and families, meteorite delivery, and planetary ring genesis and evolution. An understanding of fragmentation, however complete, cannot *alone* provide the answers to these questions; it must, however, play an inseparable role in any satisfactory physical explanation.

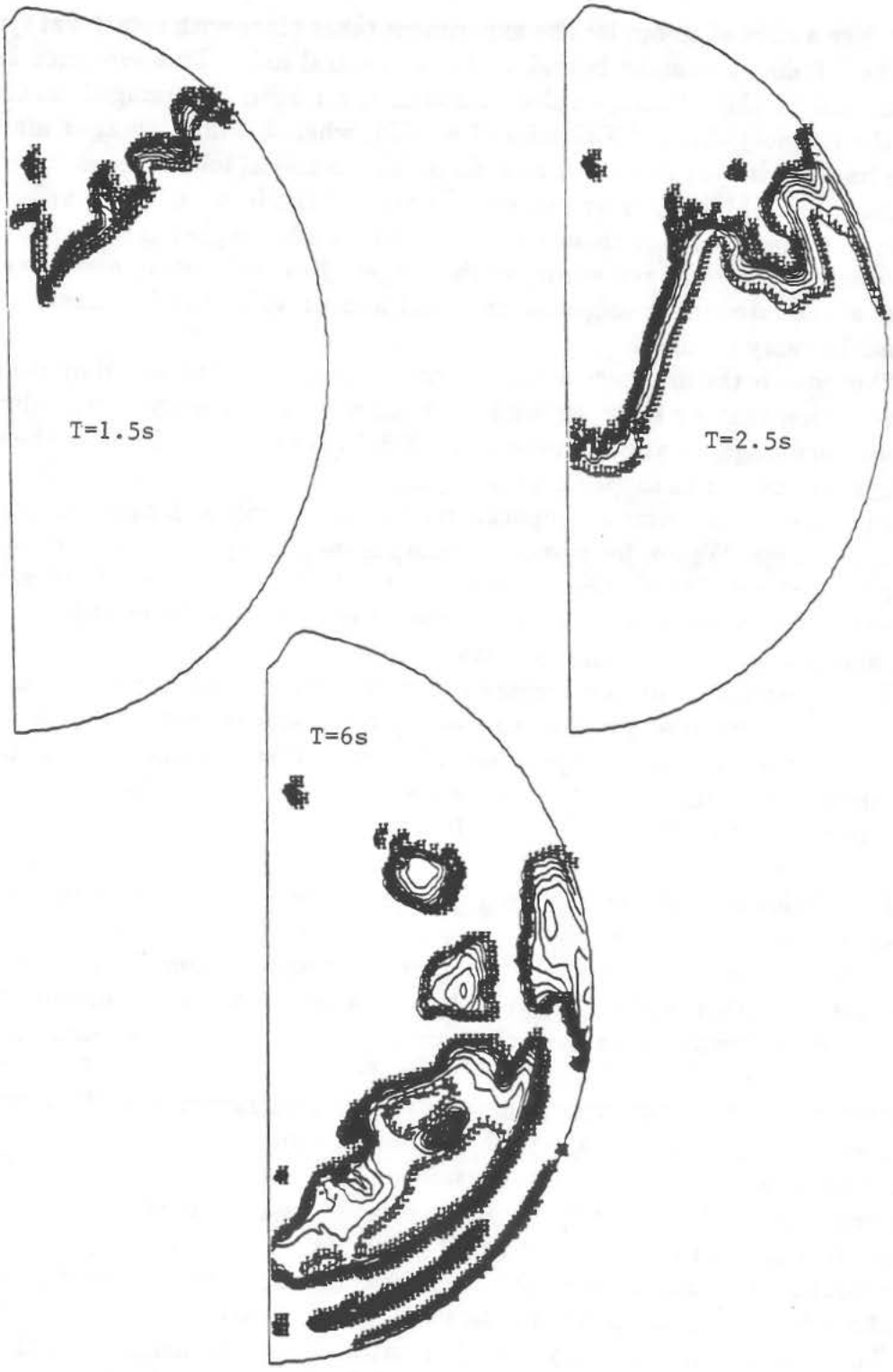

Figure 2. This simulation of the Stickney impact of Phobos illustrates a relatively non-disruptive impact event. Damage levels are contoured, representing the level of disruption of the target. The first two frames show the importance of free-surface interactions in the propagation of the damage front, while the final frame shows the remaining unfragmented regions. A more catastrophic event typically results in far greater distortions as the fragments are accelerated away from the impact.

Figure 3. A photomosaic of the Martian satellite Phobos, as imaged by one of the Viking orbiters. The prominent crater is Stickney, whose diameter (11.3 km) is actually greater than the satellite's mean radius (11.0 km). It is generally accepted that the prominent grooves, such as the ones observable to the lower right, were caused by the impact. Because Phobos may serve as a base for the manned exploration of Mars, it is important to understand what changes were brought about by this impact. Furthermore, Phobos may in fact be a captured asteroid, and could heighten our understanding of this very mysterious and important family of objects.

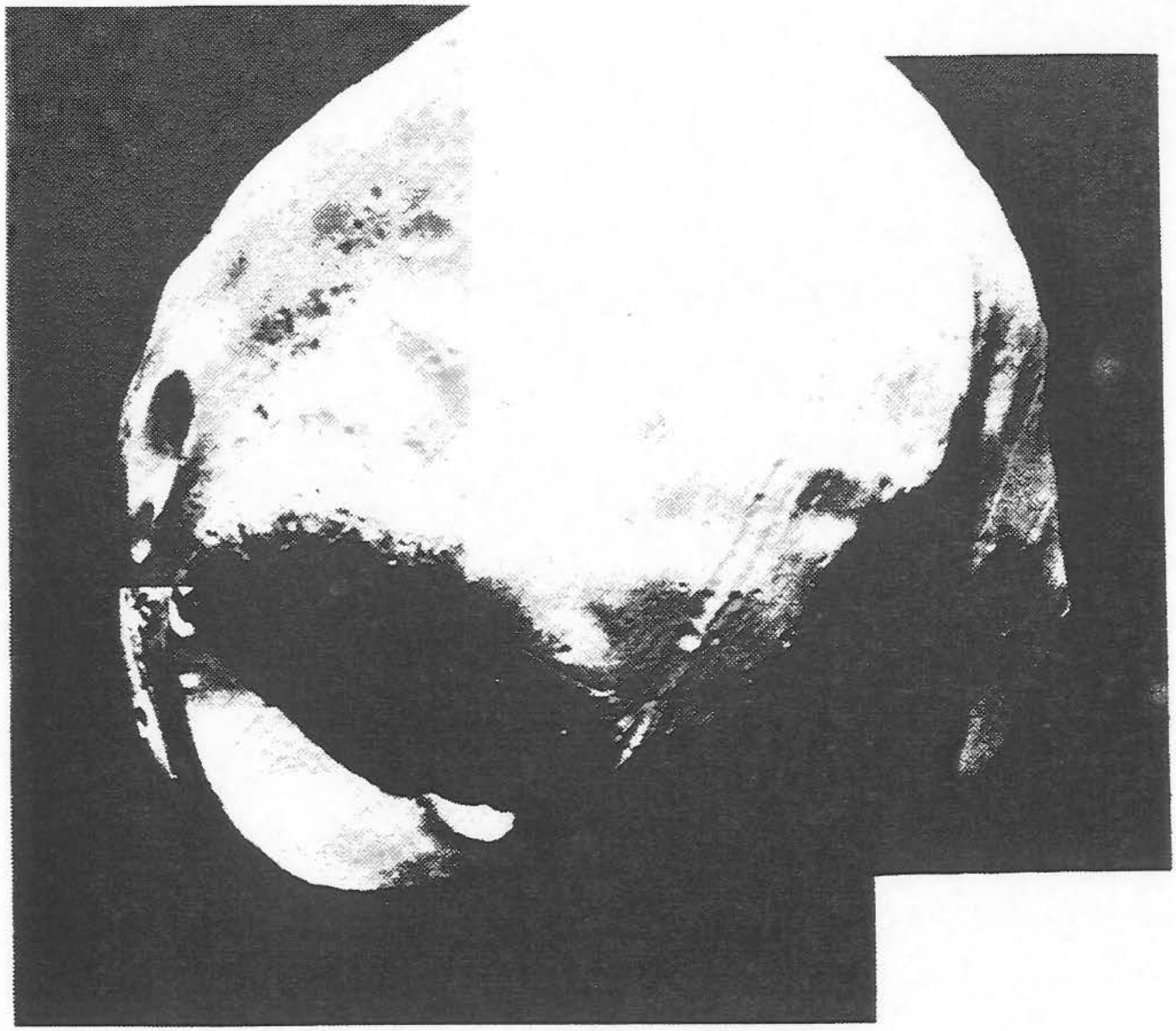

Press Abstract

ANCIENT OCEANS AND MARTIAN PALEOHYDROLOGY

by

Victor R. Baker, Robert G. Strom, Virginia C. Gulick,
Jeffrey S. Kargel, Goro Komatsu, and Vishwas S. Kale
Department of Planetary Sciences
Lunar and Planetary Laboratory
University of Arizona
Tucson, Arizona 85721

Solving the Puzzle

Science strives to make sense from the bewildering complexity of Nature. Its processes have been likened to a kind of puzzle solving in which the solution is an enhanced understanding of the natural world. Certainly one of the most perplexing puzzles of nature is that posed by the evidence of ancient water processes on the planet Mars. A century ago the fuzzy images of Mars in telescopes led some astronomers to speculate that putative intelligent inhabitants had transformed a desert planet to productive agriculture through systems of canals. During the 1960s and 1970s the high-resolution pictures returned from orbiting spacecraft revealed that the Martian "canals" were really the products of combining imperfect observations with hopeful imaginations. Nevertheless, the reality of the Martian landscape revealed by modern spacecraft pictures proved even more intriguing than the imagined scenarios.

The heavily cratered, ancient highlands of Mars are dissected by networks of valleys. Huge outflow channel systems, tens of miles wide, emanate from zones of massive collapse. Water flows are clearly indicated by the landforms associated with these features. Additional landforms indicate processes related to frozen ground ice. Such observations have led to many fascinating questions. Why did some portions of the Martian surface seem to have very low erosion rates, while other areas have forms indicating intense degradation by erosional processes? Why did numerous valleys and channels form during the Martian past, when the modern climate is too cold and dry for active water flow? How could water have moved to replenish ancient streams when the modern atmosphere has less than 1/100 the pressure of that on Earth?

In 1990, at the 21st Lunar and Planetary Science Conference, we reported on a conceptual scheme that tied together the diverse water-related landforms of Mars. Our work partly derived from that of others who hypothesized the existence of large bodies of water on Mars during its ancient past. Evidence for a great northern ocean, which we named Oceanus Borealis, was most impressively assembled in 1989 by T.J. Parker, R.S. Saunders, and D.M. Schneeberger of the Jet Propulsion Laboratory, California Institute of Technology. Stimulated by their work and by a vast array of studies by many planetary geologists, we developed the following global model of ocean formation on Mars.

Mars Climate Model

Models are theoretical simplifications of how scientists perceive the operation of phenomena. Our model arose intuitively from experience with Martian phenomena and from hypothesizing the origin and consequences of an ocean. The following events are not yet conclusively proven, but we find them scientifically compelling.

During later Martian history huge amounts of molten rock (magma) were concentrated at one local region of the planet, the Tharsis volcano area. Massive and rapid emplacement of magma beneath this bulging hot spot melted huge amounts of ground ice, driving it into fractures on the margins of the Tharsis bulge. The water burst on to the surface at great outflow channels heading at these fractures. Driven by volcanic heat, the cataclysmic outburst floods of water eventually reached the northern plains of Mars, inundating low-lying areas to form a temporary water body, the Oceanus Borealis.

The cataclysmic ocean formation led to profound climatic changes. Dissolved carbon dioxide was released from ground water and melted ground ice. Additional carbon dioxide was released to the Martian atmosphere as relatively warm water soaked into cold soils containing adsorbed carbon dioxide. Carbon dioxide previously frozen in the northern polar cap would also enter the atmosphere. This cataclysmic release of carbon dioxide profoundly changed the atmospheric heat balance, allowing the penetration of solar radiation but trapping much of the resulting heat released by the planetary surface. The planetary warming that ensued is exactly of

the sort presently exacerbated on Earth because of the burning of fossil fuels to release carbon dioxide. On Mars, however, this "greenhouse effect" was further enhanced by massive evaporation of water from the ancient floods and the transient ocean.

Water vapor is also an extremely potent greenhouse gas. As Martian temperature rose, water, frozen in upland permafrost, was released to flow into lakes or the Oceanus Borealis. The climate moved to a maritime state, with precipitation possible. This maritime state was a temporary warm, wet interval, perhaps lasting only thousands or a few million years. When the oceans gradually evaporated or froze, the planet returned to its cold, dry conditions with its water trapped as ground ice in underground permafrost. It is this cold, dry mode which presently characterizes Mars.

During the late phase of ocean formation, much of the precipitation fell as snow. Particularly near the south pole and in upland areas, the snow accumulated and was transformed to ice. As the snow and ice built up to sufficient thickness, it eventually flowed as glaciers. The epoch of glacier formation was probably relatively short on the planetary time scale of billions of years.

We hypothesize that Oceanus Borealis was probably a persistent feature during the first billion years or so of Martian history. At that time the planet was experiencing a relatively high rate of impacting objects. The dense water and carbon dioxide atmosphere allowed precipitation as rain, resulting in the widespread valley networks of the Martian uplands. However, water was being lost because of dissociation in the upper atmosphere of the planet. The hydrogen was lost to space while the oxygen contributed to the red color of the planet by oxidizing various materials. Eventually water loss and precipitation of the carbon dioxide as carbonate rock reduced the atmospheric pressure below the greenhouse level for maintaining the ocean. Most of the water was sequestered into the very permeable rocks of the planet where it comprised ice in a permafrost.

The ocean was able to reform much later in the planet's history because of the Tharsis volcanism described above. This cataclysmic ocean was smaller than the original because of the water loss by hydrogen escape. However, it was big enough to temporarily modify the climate, producing the enigmas that had bothered us about the Martian surface.

Outrageous Hypotheses

Sometimes science is viewed as a monolithic enterprise of computers, laboratory equipment, and individual theorists. We forget that science is a group exercise in which people make sense, a kind of common sense, out of the world in which they live.

We feel that the above model makes sense out of what previously seemed to be perplexing problems of past environmental change on the planet Mars. Our model is really an elaborate scientific hypothesis that is contrary to previous theories of climatic change and geological evolution for Mars. Thus, it is an "outrageous hypothesis," but the outrage is not upon factual observations but rather to theoretical beliefs held by many Mars scientists. Whether or not this new view prevails will depend upon how well it explains otherwise enigmatic phenomena.

Our studies of impact crater densities on certain Martian landforms show that late in Martian history there could have been coincident formation of (1) glacial features in the southern hemisphere, (2) ponded water and related ice features in the northern plains ("Oceanus Borealis"), (3) fluvial runoff on Martian uplands, and (4) active ice-related mass-movement. The numerous landforms could, of course, be ascribed to unique, separate causes. However, our model of transient ocean formation ties these diverse observations together in a long-term cyclic scheme of global planetary operation. Geologists long ago demonstrated that Earth processes follow such cyclic operation, and we extend that concept to Mars.

If our "outrageous hypothesis" proves correct, it will provide a new confidence on how Mars works as a planet. It will especially illuminate how Martian water-related systems have evolved through time. We need a similar confidence for Earth. Rather than idealized future "scenarios" given to us by computers, we need an understanding of how the whole planet works. If we can figure this out for a slightly smaller, slightly colder version of Earth known as Mars, that process of common sense should allow us the same revelation about Earth and its global changes. As the philosopher William Clifford once said of science, "... the truth at which it arrives is not that which we can ideally contemplate without error, but that which we may act upon without fear."

INTERSTELLAR GRAINS WITHIN INTERSTELLAR GRAINS;

Thomas J. Bernatowicz[1], Sachiko Amari[2,1], Ernst K. Zinner[1] and Roy S. Lewis[2]; [1]*McDonnell Center for the Space Sciences & Physics Department, Washington University, St. Louis MO 63130-4899, USA ;* [2]*Enrico Fermi Institute & Dept. of Chemistry, University of Chicago, Chicago IL 60637-1433, USA.*

In this paper we report the discovery of crystals of titanium carbide in an interstellar graphite spherule. The titanium carbide is another species in the growing list of interstellar grains which have been discovered in chemically processed samples of primitive meteorites. The new species is particularly interesting in that it has come to us in a protective wrapping (the graphite spherule) which has eliminated the possibility of chemical alteration during its residence in the interstellar medium and in the meteorite in which it was discovered. It thus looks today just as it did when it formed in the atmosphere of some carbon-rich star, at a time before the sun and the planets came into existence.

For more than a half century astronomers have been aware of the presence of interstellar dust from its obscuring effects on the light from stars. From various kinds of studies they have also been able to divine some notion of its composition and particle sizes. Large clouds of interstellar dust and gas can gravitationally collapse to form new stars. Nuclear reactions within these new stars alter the composition of the original gas and dust constituents, and stellar winds spew this altered material back into the interstellar medium. Thus, the chemical composition of the galaxy evolves with time.

Cosmochemists have long known that the sun and the planets owe their particular compositions to a mixture of interstellar gas and dust, but it was thought until fairly recently that all vestiges of the original constituents had been erased by complete homogenization of the dust component very early in the formation of our solar system. The evidence for this idea was based on the observation that the isotope composition of the more abundant elements was the same regardless of whether one was making measurements on a terrestrial rock, a moon rock or a meteorite. Any differences that were observed were usually explicable as the result of well-understood nuclear and chemical processes that occur within the solar system. However, some poorly understood variations in isotope composition occurred in the noble gases, which are generally present in very low abundances in solid materials. It was in an effort to isolate the mineral carriers of these noble gases that Edward Anders and his colleagues at the University of Chicago began nearly two decades ago to chemically treat primitive meteorites in order to dissolve away unwanted minerals and concentrate the carriers of unusual neon and xenon. These chemical processing procedures eventually led to the discovery of meteorite grains which could unambiguously be pronounced as stardust -- grains which condensed in the atmospheres of diverse types of stars, were

expelled from these atmospheres and existed for a time as interstellar grains, and which finally were incorporated into the interstellar cloud from which our solar system formed, but nonetheless had survived all of these tumultuous events.

To date, small interstellar grains of diamond, silicon carbide and graphite have been found. It is fair to ask how we can be confident that these grains really are stellar condensates, and not simply minerals that formed in our own solar system. Because of advances in microanalytical techniques, it is possible to measure the isotope composition of some abundant elements in individual grains, many of which are so small as to be invisible to the naked eye. We find that the compositions of some are dramatically different from the average solar system composition. For example, in typical solar system material, variations of a few percent in the proportions of the two carbon isotopes ^{12}C and ^{13}C would normally be considered large; but in individual interstellar carbon grains the proportions can be as much as fifty times the solar system average value. This difference is comprehensible if we consider that carbon in the solar system represents an average of carbon from many different stars, while an individual interstellar graphite grain represents only the carbon from one particular star, which need not have carbon isotope abundances similar to this average.

In our current work we have combined isotope studies of individual interstellar graphite grains from the Murchison meteorite with studies of the interiors of these grains with the transmission electron microscope (TEM). These grains are very small (only a few thousandths of a millimeter in size), yet after isotope measurements it is nonetheless possible to pick up a particle with delicate apparatus, imbed it in a special hard resin, and slice it, using a microtome with a diamond blade, into dozens of wafers, each only several hundred atoms thick. This is necessary because, even though the particles are very small, they are too thick to be studied in the TEM. Once such slices have been obtained, it is possible to view features of the grain even down to the size of individual layers of atoms.

The graphite particles are roughly spherical in shape, and have two basic kinds of internal structure. In one type, the graphite is arranged in circular layers, much like the inside of an onion. In the other type of interstellar graphite, the structure is that of a ball of small scales. Both kinds of structure are peculiar, and not observed in terrestrial graphite. An unexpected but very exciting discovery was the presence of small crystals, a hundred or so atomic diameters in size, within one of the scaly graphite particles. In addition to getting pictures of the crystal lattice structure of the included crystals, we could also study their composition and crystal structure in the TEM, and from these studies we learned that the crystals are titanium carbide, a mineral not previously found in meteorites.

Chemical equilibrium calculations made in 1978 by Lattimer, Schramm and Grossman at the University of Chicago had in fact predicted that these two minerals, graphite and titanium carbide, would be the first to condense in the atmosphere of a carbon-rich star. According to their calculations, graphite should condense first, followed by titanium carbide, at temperatures of 1200-1700 degrees Celsius. The fact that we observed titanium carbide crystals *inside* of the graphite must mean that the growth of graphite was somewhat delayed from what calculations based on chemical equilibrium suggest--an effect which had also been predicted by some astronomers. From studying the internal structure of the interstellar graphite spherules and the included titanium carbide we can make some educated guesses about the formation of the spherules. First, they probably formed at high temperatures and were the first grains to condense in their particular stellar atmospheres; second, they may have formed relatively rapidly (possibly in times measured in days, for example), since the graphite layers are often not very well developed, as they would be expected to be if condensation proceeded slowly; third, the grains may have been expelled from their stars to regions of substantially lower gas pressure (interstellar space?), since we don't find the other minerals which would have condensed after graphite and titanium carbide.

No one has yet observed titanium carbide by conventional astronomical measurements of stars or the interstellar medium. This is perhaps not surprising, since this mineral comprises only a few parts per million of one of the graphite spherules we studied. But it points out that the laboratory study of interstellar grains extracted from primitive meteorites may yield a far richer and more complete picture of how such grains form than can be gotten from astronomical study alone. The laboratory observations also pose interesting challenges to theoreticians who model the chemistry of stars and the formation of solid grains in their atmospheres.

K/T AGE FOR THE POPIGAI IMPACT EVENT?; A.L. Deino, Geochronology Center, Institute of Human Origins, 2453 Ridge Road, Berkeley, CA 94709, J.B. Garvin, NASA/GSFC, Geodynamics Branch, Code 621, Greenbelt, MD 20771, S. Montanari, Dept. of Geology and Geophysics, U.C. Berkeley, Berkeley, CA 94720.

The multi-ringed POPIGAI structure, with an outer ring diameter of over 100 km (analysis of a digital elevation model for the region by Garvin and others suggests 105 km), is the largest impact feature currently recognized on Earth with an Phanerozoic age [1]. The shallow depression which defines the structure occurs in the taiga of north-central Siberia within the Anabar crystalline shield. The target rocks in this relatively unglaciated region consist of upper Proterozoic through Mesozoic platform sediments and igneous rocks overlying Precambrian crystalline basement. Extensive field studies by Masaitis and colleagues [1], many of which are unpublished (Masaitis, 1989, pers. comm.), suggests that huge sheets of impact melt are preserved within the outer ring which defining the structure, and as isolated deposits of ejecta to the southwest beyond the rim. The apparent volume of the present-day structure exceeds 1000 cubic km, with a depth/Diameter ratio of only 0.004. The maximum present-day depth of the structure is only ~ 400 m, a factor of at least 5 smaller than the predicted pre-erosional depth; this suggests that over 1000 cubic km of materials may have been excavated by the impact event, with at least 100 cubic km of internal impact melt.

The reported absolute age of the Popigai impact event is 39 ± 9 Ma (K-Ar) [1], 38.9 (average of K-Ar ages) [2], and 30.5 ± 1.2 Ma (fission-track) [3]. With the intent of refining this age estimate for comparison to Eocene/Oligocene marine microtektites, a melt-breccia (suevite) sample from the inner regions of the Popigai structure provided to JBG by V. Masaitis was prepared for total fusion and step-wise heating $^{40}Ar/^{39}Ar$ analysis.

Sample #74034 (V. Masaitis designation) is a suevitic grayish-brown rock, somewhat vesicular, with abundant round to sub-round clasts 0.5 to 0.8 cm in diameter, within a clastic-appearing matrix (grain size less than 0.3 mm). Smaller glassy clasts grade into the matrix. The glass is translucent green, dark green to black, occasionally vesicular, or tan with pronounced vesicles, as well as vitreous gray or clear. The dark green to black glass clasts have textures apparently associated with schlieren (flowing or stretching, as evidenced by the stretched vesicles). In addition, there appear to be mineral clasts which are either clear or milk white in color. The gray, white, or colorless mineral clasts are mostly quartz with occasional potassium feldspar (mostly in the darker schlieren clasts). Some quartz grains exhibit multiple sets of shock lamellae.

Middle infrared emission/reflectance spectroscopic analysis of a range of features observed within the sample suggest the presence of fused silica (lechatelierite?), silica glass, and a component of obsidian-like glass (felsic, perhaps melted K-spar). Fig. 1 is a plot of several representative hemispherical mid-IR reflectance spectra for sub-regions of the sample. Our conclusion is that sample #74034 represents a typical heterogeneous suevite from the crater interior (fall-back ejecta mixed with impact melt).

The major and minor element composition of the vesicular glass has been analyzed with the electron microprobe along eight 100 micron transects within a thin section. With the exception of one transect that intersected glass with a K-feldspar composition, the glass shows only slight compositional variation, and is practically anhydrous as indicated by microprobe totals generally greater than 99%. The general range of glass composition is 60% to 61.5% SiO_2, 0.7% to 1.0% TiO_2, 16% to 17.3% Al_2O_3, 4.1% to 4.8% MgO, 3.4% to 4% CaO, 0% to 0.2% MnO, 6.3% to 7.1% FeO, 2.0% to 2.3% Na_2O, and 2.3% to 2.9% K_2O.

Glass fragments separated from this sample have been dated by the laser-fusion $^{40}Ar/^{39}Ar$ technique. Our initial experiments consisted of five total-fusion analyses of individual 90 to 260 microgram grains, which yielded ages of 52.2, 59.0, 64.2, 64.4, and 65.9 Ma with 1σ analytical errors of about 0.2 Ma. All of these yielded >98% $^{40}Ar^*$, suggesting that very little alteration has affected the glass. We also performed a preliminary 7-step incremental-heating experiment on approximately 350 microgram of sample (Fig. 2). About 72% of the ^{39}Ar release from this sample yielded ages between ~65–68 Ma, while the remainder was contained in an abrupt 'hump' reaching a maximum of 243 Ma at about one-third of the ^{39}Ar released. The integrated total-fusion age of this experiment is 77.7 ± 0.5 Ma, with a 'plateau' (of only three steps but 58% of the gas) of 65.5 ± 0.5 Ma. A much more detailed spectra of 38 release steps showing generally similar behavior to the first experiment was subsequently obtained from 1.57 mg of sample. This spectra started off with an apparent age of (coincidentally?) 242 Ma, followed by a rapid decrease to a loosely defined 'plateau' ranging between ~72 and 60 Ma, and a mean of 65.4 ± 0.3 Ma. Aside from the initial release, the spectra is characterized by a broad hump again reaching a maximum within the first half of gas release. The integrated total-fusion age of this spectra is 66.3 ± 0.4.

Although the total fusion and step-heating experiments suggest some degree of age heterogeneity, the recurring theme is an age of around 64 to 66 Ma. There is no suggestion of a late Eocene age component similar to that of previous K-Ar and fission-track dating results from Popigai samples. We cannot explain this discrepancy except to postulate 1) either that the prior results are incorrect, or 2) that the glass of sample #74034 contains a more or less uniformly distributed quantity of initial argon inherited from the target rocks. However, this sample consists of unaltered, non-hydrated, vesicular (likely degassed) moderately-high-potassium melt glass. If correct, the new ages suggest that the Popigai impact event is approximately the age of the K/T boundary (66 Ma; [4]). We would stress, though, that these results are preliminary since they were obtained from one sample only. They must be corroborated by analysis of additional high-quality samples of suevites and tagamites from throughout the crater area.

Acknowledgements: We gratefully thank V.L. Masaitis of the Ministry of Geology in Leningrad, USSR (VSEGEI) for providing us with sample #74034 for analysis.

K/T AGE FOR THE POPIGAI IMPACT EVENT?; Deino A.L. et al.

References:
[1] Masaitis V. L. et al. (1975) *The Popigai meteorite crater*, Nauka Press, Moscow, USSR, 123 pp. (English translation in NASA TT F-1, no. 900, 171 pp.)
[2] Masaitis V. L. et al. (1980) *The geology of astroblems*, "Nedra" Press, Leningrad, USSR, 231 pp. (English translation in NASA TM-77743)
[3] Storzer D. and G. Wagner (1979) Fission track dating of Elgygytgyn, Popigai, and Zhamanshin impact craters: No sources for Australasian or North-American tektites; *Meteoritics* 14, no. 4, p. 541-542.
[4] Obradovich, J., and Sutter, J. (1984) What is the age of the Cretaceous-Tertiary boundary as recorded in continental rocks?; Geol. Soc. Amer. Abs. 16:612.

Fig. 1

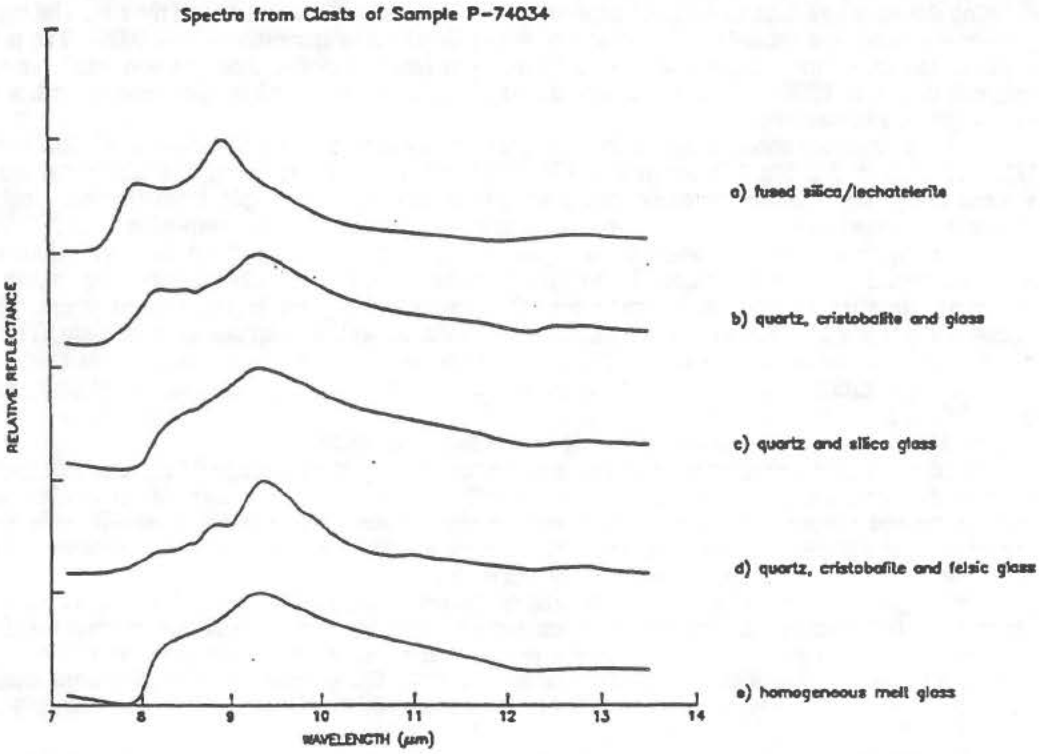

Fig. 2

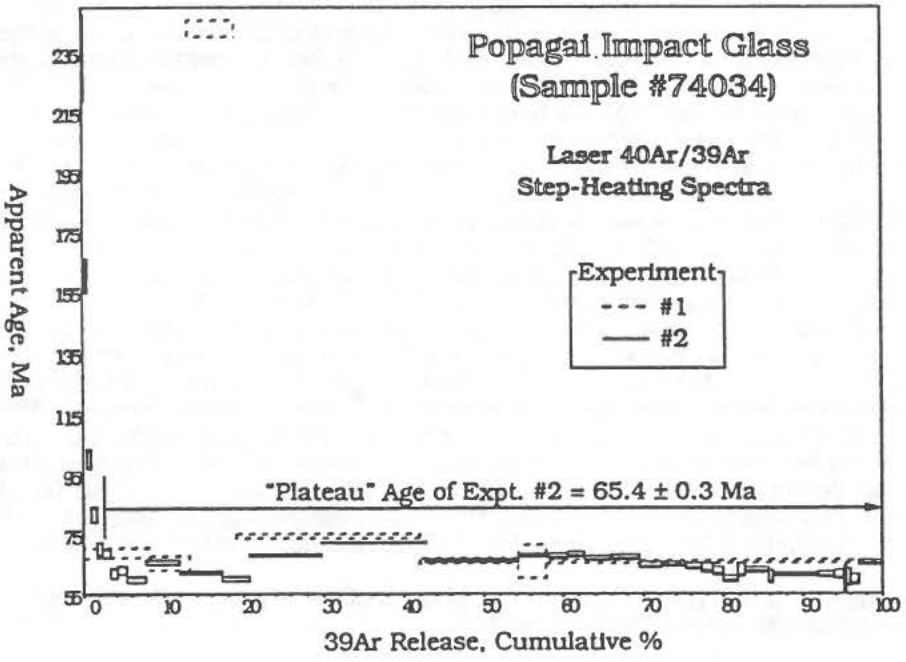

LUNAR MARIA AND RELATED DEPOSITS: PRELIMINARY GALILEO IMAGING RESULTS *R. Greeley*[1], *M. Belton*[2], *L. Bolef*[1], *M. Carr*[3], *C. Chapman*[4], *M. Davies*[5], *L. Doose*[6], *F. Fanale*[7], *L. Gaddis*[1], *R. Greenberg*[6], *J. Head*[8], *H. Hoffman*[9], *R. Jauman*[9], *T. Johnson*[10], *K. Klaasen*[10], *R. Koloord*[6], *A. McEwen*[11], *S. Murchie*[8], *G. Neukum*[9], *J. Oberst*[9], *C. Pieters*[8], *C. Pilcher*[12], *J. Plutchak*[8], *M. Robinson*[6], *R. Sullivan*[1], *J. Sunshine*[8], *J. Veverka*[13] 1. Ariz St U, Tempe, AZ. 2. NOAO, Tucson, AZ. 3. USGS, Menlo Park, CA. 4. PSI, Tucson, AZ. 5. Rand, Santa Monica, CA. 6. U AZ, Tucson, AZ. 7. U Hawaii, Manoa, HI. 8. Brown U, Providence, RI. 9. DLR, Munich, Germany. 10. JPL, Pasadena, CA. 11. USGS, Flagstaff, AZ. 12. NASA, Washington, D.C. 13. Cornell U, Ithaca, NY.

During the Earth-Moon flyby the Galileo Solid State Imaging (SSI) system (1) obtained new information on lunar maria. Imaging data in 7 spectral bands (0.4 to 1.0 μm wavelength) provide color data for deposits on the western limb, including the Orientale basin (2) and part of the farside (3). General objectives were to determine the composition and stratigraphy of mare and related deposits for areas not previously seen well (or at all) in color, and to compare the results with well-studied nearside maria (4). The imaging sequence began with observations of the Apollo 12 and 14 landing sites and extended west to include Oceanus Procellarum and the Humorum basin. This sequence enabled relative calibration of Galileo data using previous earthbased multispectral observations and spectral data obtained from Apollo samples. A later imaging sequence extended around the western limb and provided new color data for mare deposits in the Orientale basin and those associated with the craters Grimaldi, Riccioli, and Schickard. The last imaging sequence covered part of the farside and included mare deposits in the Apollo basin, light plain deposits such as those in the Korolev basin, and dark mantle (pyroclastic?) materials.

Initial results from images reduced with preliminary calibrations show that Galileo spectral reflectance data are consistent with previous earthbased observations. Color visualization images were prepared from ratios of Galileo SSI filter data (violet/0.76→blue, 0.76/violet→red; 0.76/IR→green) in order to assess the relative titanium (blue is relatively high Ti, red is relatively low Ti) and mafic content of maria. Galileo results are comparable to those derived from earthbased spectra for Oceanus Procellarum (7) and Humorum (8). The relative color of mare units correlates with photogeologic features and the titanium content as determined from lunar samples (5 and reviewed by 6). These areas and the general western nearside maria are highly complex and include volcanic centers of the Rümker Hills, Marius Hills, and Aristarchus Plateau (9-14). Mare units in these areas also have a wide range of titanium contents (15) and ages (16). Galileo data show the compositional complexity of western nearside maria and demonstrate that calibrated images can be used to map the color of maria on the farside and in limb areas not readily seen from Earth such as regions of the western limb. For example, small deposits of Imbrian-age lavas are seen on the western margin of Oceanus Procellarum. Galileo data suggest that these deposits consist of relatively bluer flows that were erupted early in the emplacement of lavas in the area. Also seen on the western limb are the impact structures Grimaldi, Riccioli, and Schickard. Grimaldi is a 430 km basin centered at 5° S, 68° W and contains a 230 km ring filled with mare deposits of Eratosthenian age. It is a major mascon mare (17, 18). Riccioli is a 146 km crater superposed on the northwestern part of the outer ring of Grimaldi; patches of mare deposits (undated) occur on the floor and in the northern half of Riccioli. Irregular depressions in the mare deposits may indicate subsidence of lava lakes (19). Galileo SSI data distinguish the mare deposits associated with Grimaldi and Riccioli.

Schickard is a 227 km basin centered at 44° S, 55° W. Unlike most lunar structures of this size, it has no apparent ring or central peak complex. It is filled with light plains material and mare deposits of Imbrian age. The light plains may represent ejecta from the Orientale basin (6). Galileo color data for Schickard maria are consistent with previous spectral reflectance measurements, showing an intermediate (violet/0.76) color. In addition, a strong mafic component is seen around Schickard and extends as a large regional patch southeast toward Schiller. This area corresponds to the zone proposed to be an older mare deposit now mantled by light plains (20,

28). It was suggested that dark halo craters excavated basaltic materials from beneath the light plains and Galileo results support this model.

Mare deposits in the Orientale basin include Mare Orientale, Lacus Veris (between the Inner and Outer Rook Mountains), and Lacus Autumni (between the Outer Rook and Cordillera Mountains), as described by (23-25). Earthbased spectral reflectance data obtained by Spudis et al. (26) suggest that Lacus Veris and Lacus Autumni are "contaminated" by material derived from the local highlands. Except for this mixing, they proposed that the mare deposits are similar in composition to nearside maria. Galileo spectral reflectance data show heterogeneities in Mare Orientale, with the eastern region being more Ti-rich than the western region.

Apollo is a 505 km basin containing a central ring 250 km across, centered at 36°S, 151°W. A partial third ring has also been described (6). Patches of maria fill parts of the Apollo basin. The superposition of Apollo on the rim of the South Polar-Aitken basin may have enhanced the eruption of mare lavas (10). Galileo SSI data distinguish the mare deposits, but await further calibration before assessment of composition. The general area within the South Pole-Aitken basin shows a strong mafic component. This signature can be attributed to iron-rich material excavated from the lower crust or upper mantle, or to the presence of a cryptomaria. The possible cryptomare deposits in both the South Polar and Schickard basins may represent very early volcanism on the Moon.

Dark mantle deposits are seen in the Aristarchus Plateau, southeast of Copernicus, and in the Orientale basin. Consistent with earthbased observations (29, 30), Galileo data show the Aristarchus deposits to be similar to Apollo 17 orange glass whereas the deposits southeast of Copernicus are similar to the Apollo 17 black glass deposits. Dark mantle deposits on the southwestern part of the Orientale basin form a ring about 200 km in diameter. Galileo data suggest that these presumed pyroclastic deposits have closer affinities with the black glasses found at the Apollo 17 site than the orange glass.

In the mid 1970s a simple two-fold model of mare basalts was developed that involved high and low titanium lavas; it was thought that low titanium lavas erupted during early lunar volcanic history from shallow magma chambers, and that high titanium lavas were erupted later from deeper sources. Subsequently, it was recognized that mare lavas have a wide range of titanium content and neither their ages nor depth of origin correlate well with titanium content. Galileo results confirm this complexity. The preliminary results presented here are given in qualitative terms relative to earthbased observations of the Oceanus Procellarum-Humorum region. Calibration efforts currently underway (3, 27) should lead to quantitative spectral reflectance data obtained from the Galileo images for extrapolation to the lunar western limb and farside.

1. Belton, M.J.S. et al., 1991 (this vol.) 2. Head, J.W. et al., 1991 (this vol.) 3. Pieters, C.M. et al., 1991 (this vol.) 4. Fanale, F., 1990. EOS, Dec 8. 1803-1804 5. Pieters, C.M., 1978. *Proc. Lunar Planet. Sci. Conf. 9.* 2825-2849 6. Wilhelms, D.E., 1987. *U.S. Geol. Surv. Prof. Paper* 1348 302 p 7. Pieters, C.M. et al., 1980. *J. Geophys. Res.*, 85. 3913-3938 8. Pieters, C.M., et al., 1975. *Proc. Lunar Sci. Conf. 6.* 2689-2710 9. Guest, J.E., 1971. *Geo. and Phys. of the Moon.* Ch. 4. 41-53 10. Head, J.W., 1976. *Rev. Geophys. and Space Phys.* 14. 265-300 11. Head, J.W., Gifford, A., 1980. *Moon and Planets* 22. 235-258 12. Whitford-Stark, J., Head J.W., 1977. *Proc. Lunar Planet. Sci. Conf. 8.* 2705-2724 13. Whitford-Stark, J., Head J.W., 1980. *J. Geophys. Res., 85.* 6579-6609 14. Greeley, R., Spudis, P.D., 1978. *Proc. Lunar Planet. Sci. Conf. 9.* 3333-3349 15. Papike, J.J., Vaniman, D.T., 1978. *Geophys. Res. Lett.* 5. 433-436 16. Boyce, J., 1976. *Proc. Lunar Planet. Sci. Conf. 7.* 2717-2728 17. Sjogren, W.L. et al., 1974. *The Moon, 9.* 115-128 18. Solomon, S.C., Head, J.W., 1980. *Rev. Geophys. and Space Phys.*, 18. 107-141 19. Schultz, P.H., 1976. *Moon Morphology.* U. Texas Press 20. Hawke, B.R., Bell, J.F., 1981. *Proc. Lunar Planet. Sci. 12b.* 665-678 21. Head, J.W., 1974. *The Moon 11.* 327-356 22. Moore, H.J. et al., 1974. *Proc. Lunar Sci. Conf. 5.* 71-100 23. Greeley, R., 1976. *Proc. Lunar Sci. Conf. 7.* 2747-2759 24. McCauley, J.F., 1977. *Phys. Earth Planet. Int. 15.* 220-250 25. Scott, D.H. et al.,1977. *USGS Misc. Invest. Map I-1034* 26. Spudis, P.D. et al., 1984. *J. Geophys. Res.* 89. C197-C210 27. McEwen A. et al., 1991 (this vol.) 28. Bell, J.F., Hawke, B.R., 1984. *J. Geophys. Res. 89.* 6899-6910 29. Adams, J.B. et al., 1974. *Proc. Lunar Planet. Sci.* 5. 171-186 30. Gaddis, L.R. et al., 1985. *Icarus, 61.* 461-489.

MARS RADAR MAPPING: STRONG DEPOLARIZED ECHOES FROM THE ELYSIUM/AMAZONIS OUTFLOW CHANNEL COMPLEX; J. K. Harmon, M. P. Sulzer, and P. Perillat, National Astronomy and Ionosphere Center, Arecibo, PR 00613.

A new technique has been used to make radar maps of Mars with the Arecibo radiotelescope. The observations were made during the 1990 opposition (close approach) of Mars. Among the most interesting of the preliminary results is the discovery of strong depolarized echoes from the enormous Elysium/Amazonis outflow channel complex. These strong echoes may represent rough-surface scattering off the youngest lava flows on Mars.

Measurement of the strength and angular dispersion of radar scattering from a planet's surface can provide information on the hardness and roughness of the surface. The typical echo from a planet can be broken down into two components: (1) a highly polarized "quasispecular" echo representing mirror-like reflections from the center of the apparent disk of the planet, and (2) a partially depolarized "diffuse" echo which arises from the entire visible disk and which is assumed to represent high-angle scattering off of very small (wavelength-scale) surface roughness elements. Two-dimensional mapping of the diffuse echo strength across the apparent disk ("reflectivity mapping") is normally done using the so-called "delay-Doppler" technique; here each element of the echo is identified by its characteristic time delay and Doppler frequency and then assigned to that spot on the planet which corresponds to that particular delay-Doppler combination. The delay-Doppler technique has been used very successfully for Venus, although in this case the interest has not been so much in the radar scattering properties *per se* as in the fact that radar reflectivity features reveal large-scale morphological structures such as volcanoes and impact craters which otherwise would be unobservable through Venus' cloud cover. In the case of Mars, whose features are already well known from orbiter images, the objective of radar mapping is to study properties (such as wavelength-scale roughness) which are not provided by the optical images and to correlate those with known surface features. Unfortunately, the standard delay-Doppler technique used to map Venus cannot be applied to Mars because of that planet's rapid rotation. The problem arises from the fact that in order to recover the entire breadth of Mars' broad Doppler spectrum one has to sample the echo at intervals which are shorter than the delay depth of the planet, which results in a foldover or delay-confusion of the echo if one uses a standard pulse train or cyclic phase code for transmission. This limitation (called "overspreading") has discouraged Mars radar mapping efforts and it is only within the last two years that any progress in radar mapping of this planet has been made.

Radar observations made at Arecibo about a decade ago showed that the diffuse radar echo from Mars shows very strong spatial variations in strength and degree of depolarization (1,2). These were simple CW observations (Doppler only) which could not be used to make two-dimensional radar maps. However, tracking of Doppler features in these data as the planet rotated suggested that the strongest diffuse/depolarized echoes (and, by inference, the roughest surfaces) were located in the northern volcanic regions of Tharsis, Amazonis, and Elysium. By contrast, the heavily-cratered uplands terrain which covers most of the southern hemisphere of Mars was found to have a diffuse echo component which is relatively weak and featureless. In reporting those results we speculated that much of the enhanced diffuse scatter arose from rough-textured volcanic constructs and lava flows (2). This is certainly a plausible hypothesis since lava flows on Earth can be extremely rough and often show strong radar depolarization.

The first true radar maps of Mars were made by Muhleman and coworkers (3) during the 1988 opposition. They avoided the overspreading problem completely by transmitting with the Goldstone antenna in California and mapping the received echo with the Very Large Array interferometer in New Mexico. Their maps confirmed the strong Tharsis feature as well as the relative radar blandness of the heavily cratered uplands. Their data did not include a full planet rotation and only the eastern edge of Elysium was mapped. During the 1990 Mars opposition we made the first attempt to make the first delay-Doppler reflectivity maps of Mars using the "random code" or "coded long pulse" technique, a method developed to overcome the overspreading problem in ionospheric radar measurements (4,5). In this technique a random (non-repeating) code is transmitted. The resultant echo contains a delay clutter which reduces the sensitivity of the measurement but, because the code is random, does not add delay confusion. We have made about 20 observations using this

MARS RADAR MAPPING: Harmon J.K. *et al.*

technique with the S-band (12.6-cm wavelength) radar at Arecibo from September 1990 to January 1991. Although the mapping analysis is not yet complete, some interesting results have already been obtained. Of these, perhaps the most interesting is the mapping of the radar-bright features which together make up the depolarized enhancement which we had previously seen from the general region of Elysium (2). One of the maps from this region is shown in Fig. 1; this is a radar reflectivity map of the depolarized echo component, with brighter shades corresponding to stronger echoes. Superimposed on this map is a latitude-longitude grid with 10° spacing. Although this map shows the north-south ambiguity about the Doppler equator which is inherent to the delay-Doppler method, we have established from maps obtained 6° farther north that all of the prominent features in Fig. 1 actually come from north of the Doppler equator. The northernmost feature which can be discerned is a faint patch near 210°W, 25°N which coincides with the eastern flank of the volcano Elysium Mons. The brightest features on the map are concentrated between 180°W and 215°W at latitudes from 5°S to 10°N. This breaks down into three separate bright patches which we will denote Features "A" (near 210°W, 7°N), "B" (near 196°W, 2°S), and "C" (a large bow-shaped structure extending from 180°W to 200°W). These three features lie within (and, taken together, roughly delineate) the boundaries of the vast Elysium/Amazonis outflow channel complex as mapped by Tanaka (6). Tanaka argues that this province is the erosional remnant of catastrophic flooding (presumably by water) which occurred during a recent epoch. He describes the flood plains as consisting of "low-albedo material marked by light, wispy streaks." A study of the Viking photomosaic maps of this region shows that radar features "A" and "B" correspond to well-defined regions for which Tanaka's description is particularly apt. Feature "C" coincides precisely with what may be the outflow channel-proper, a continuous flow of dark streaks which the photomosaics show as starting near 195°W, 5°N, dipping down toward the equator, and then trending NE to about 175°W, 25°N.

Upon identifying the Elysium radar features with the outflow channel our first impression was that this was an interesting, if unexpected, example of enhanced radar backscatter from a non-volcanic surface. We speculated in our LPSC abstract that the scattering might be off gravels deposited by the floods. Since then a paper by Plescia (7) has appeared in the December 1990 issue of *Icarus* in which a strong case is made that the low-albedo features which dominate this region are in fact low-viscosity flood lavas which filled the pre-existing channels and flood plains. Plescia also points out that some of the identifications of lava flows in this region had been made a decade ago by Schaber (8); our radar feature "B" coincides with one of the lava flow features identified by Schaber. Plescia points out that these lavas are very young by Martian standards and therefore are of considerable interest for studies of the thermal and volcanic history of the planet. The identification of lava flows in the Elysium/Amazonis outflow channels would explain why we see enhanced radar backscatter from this region and not from the other large outflow channel complex in Chryse Planitia (which is not lava filled). It also offers support for our speculation of a few years ago that many of the strong features in the diffuse/depolarized radar echo from Mars are associated with rough volcanic surfaces such as lava flows.

References

(1) Harmon J.K., Campbell D.B., and Ostro S.J. (1982), *Icarus 52*, 171.
(2) Harmon J.K. and Ostro S.J. (1985), *Icarus 62*, 110.
(3) Muhleman D.O., Butler B., Grossman, A.W., and Slade M. (1989), *4th Intl. Conf. Mars*, Tucson, AZ.
(4) Sulzer M.P. (1986), *Radio Sci. 21*, 1033.
(5) Sulzer M.P. (1989), *Adv. Space Res. 9*, 153.
(6) Tanaka K.L. (1986), *J. Geophys. Res. 91*, E139.
(7) Plescia J.B. (1990), *Icarus 88*, 465.
(8) Schaber G.G. (1980), *Icarus 42*, 158.

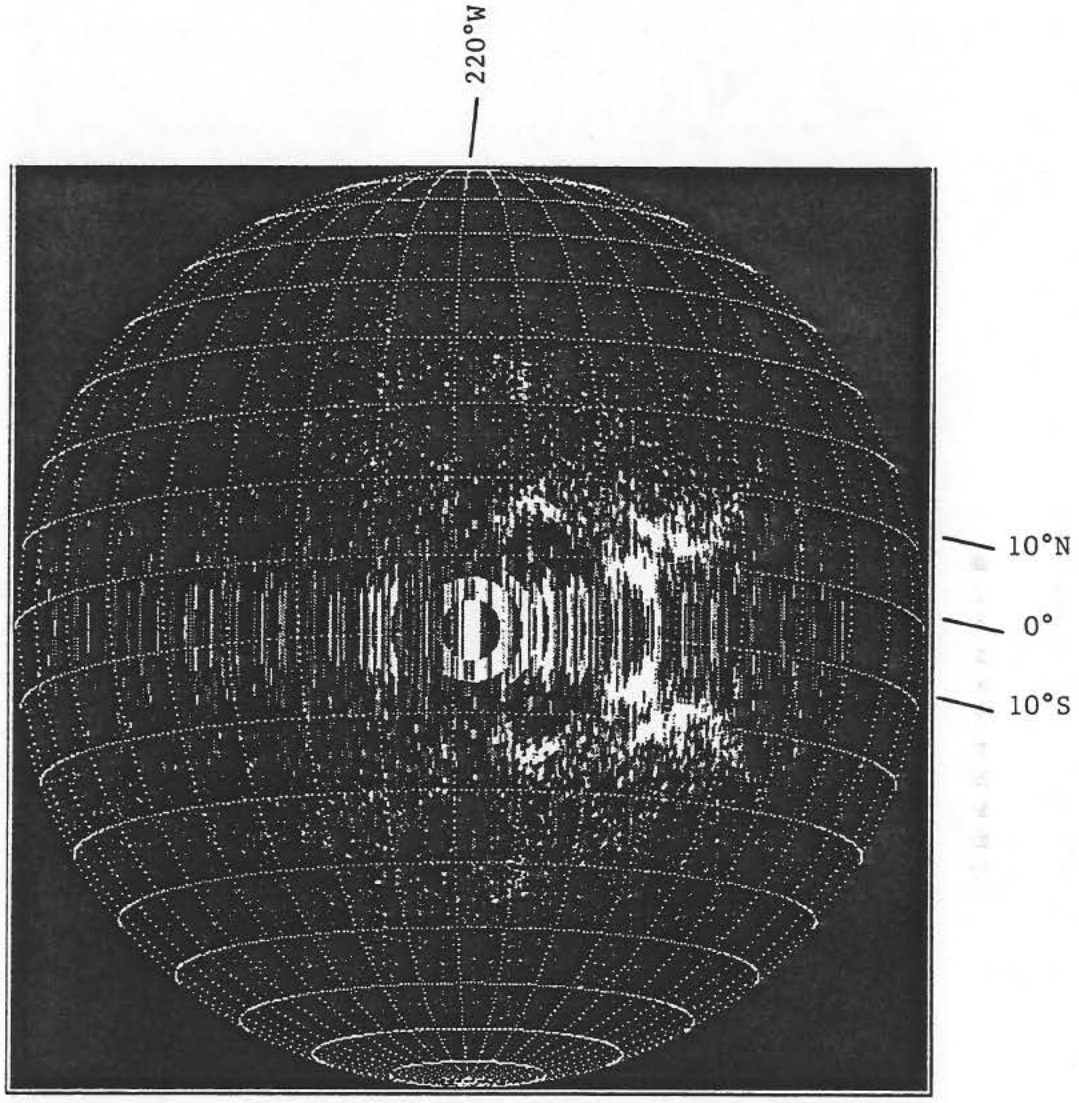

Fig. 1

ORIENTALE AND SOUTH POLE-AITKEN BASINS ON THE MOON: PRELIMINARY GALILEO IMAGING RESULTS. J. Head, E. Fischer, S. Murchie, C. Pieters, J. Plutchak, J. Sunshine (Brown University, Providence, RI, U.S.A.); M. Belton (Kitt Peak Nat. Observatory, Tucson, AZ, U.S.A.); M. Carr (USGS, Menlo Park, CA, U.S.A.); C. Chapman (Planetary Science Institute, Tucson, AZ, U.S.A.); M. Davies (RAND, Santa Monica, CA, U.S.A.); F. Fanale, M. Robinson (University of Hawaii, Honolulu, HI, U.S.A.); R. Greeley, R. Sullivan (Arizona State University, Tempe, AZ, U.S.A.); R. Greenberg (University of Arizona, Tucson, AZ, U.S.A.); P. Helfenstein, J. Veverka (Cornell University, Ithaca, NY, U.S.A.); H. Hoffmann, R. Jaumann, G. Neukum (DLR, Oberpfaffenhofen, F.R.G.); T, Johnson, K. Klaasen (JPL, Pasadena, CA, U.S.A.); A. McEwen, T. Becker (USGS, Flagstaff, AZ, U.S.A.); C. Pilcher (NASA Headquarters, Washington, D.C., U.S.A.).

On the near side of the Moon visible from Earth, the bright areas or "highlands" are composed of light-colored rock saturated with craters formed over eons by impacting meteors. Younger, less cratered, darker plains, or "mare," are composed of a thin layer of basaltic lava flows that erupted over 3 billion years ago and buried highlands-type rocks. The mare plains are concentrated into discrete, circular, topographically low regions called "basins," each of which typically also contains several concentric, ring-like belts of high mountains. Several dozen of these basins, from 300 to nearly 2000 kilometers in diameter, are filled to varying degrees with mare basalts [1,2]. The basins are thought to have formed more than 3.8 billion years ago, when the Earth, Moon, and other planets were bombarded by "leftover" asteroid-sized bodies being "swept up" gravitationally after accretion of the Solar System - hence the term "impact basins" generally applied to them [e.g., 3]. The impacting asteroids struck the Moon at velocities of around 20 km/s, excavating cavities hundreds of kilometers in diameter that penetrated deep into and perhaps even below the lunar crust. These fresh cavities promptly collapsed back in on themselves, perhaps through some combination of slumping of the cavity walls and rebound of the floors [4, 5, and others], creating the concentric belts of mountains or "basin rings."

The Imbrium basin, located in the northwestern part of the near side, has been recognized for nearly 100 years as one of the clearest examples of this type of feature [1,3,6,7,8,9,10]. An outer mountain ring, nearly 1200 km in diameter, marks a "step down" topographically from the surrounding highlands. The basaltic flows composing Mare Imbrium mostly fill the enclosed topographic depression. The interior of the mare plain also contains two well developed concentric belts of high mountains 700 and 900 km in diameter. These mountains are composed of light-colored rock like the highlands, and protrude from beneath the layers of basalt flows.

Like the Imbrium basin, most parts of other large near side basins were also buried by mare lavas that flooded in through fractures in the basin floors over the next several hundred million years. This obscured most of the original structure of the basins, including rocks excavated from tens-of-kilometers depths. Many questions about the formation and evolution of these basins, and about the nature of the lower crustal or upper mantle rocks possibly exposed within them, could be addressed if the obscuring cover of mare could be "seen through": What kinds of rocks form the inner regions of the impact basins? Are they monotonously similar from place to place, as suggested by the bland light color of highland rocks, or are there different types of rocks produced by a complex history of geologic activity? Are they like the rocks composing the highlands or are they different, providing a sample of the Moon's interior below its light-colored crust? What sequence of geologic events shaped the basins' floors and the rings of mountains in their interiors? These issues are pertinent not only to understanding lunar geology, but also to understanding the early evolution of the Earth. Our planet's geologic record of this early period has long been erased by erosion, volcanism, and plate tectonic processes, but the Earth like the Moon must also have experienced the fracturing and churning of its crust caused by basin formation. Understanding how these processes affected the Moon helps us to understand what role basin formation may have had in the Earth's earliest geologic evolution.

The Orientale basin, located at the western limb of the near side and in the adjacent portion of the far side, provides a "window" into the interior of a large impact basin. Orientale is the youngest and best-preserved of all the large lunar basins, and unlike the near side basins it contains only a patchy, discontinuous cover of mare lavas. Thus its interior structure and its deeply excavated rocks are visible at the lunar surface [3,8,10,11,12,13]. The Orientale basin was in the sunlit portion of the Moon during the flyby of *Galileo* through the Earth-Moon system on December 7-8, 1990 [14,15], and it was imaged with a resolution of 3 km by the spacecraft's Solid-State Imaging (SSI) camera. The SSI camera has seven color filters covering the wavelength range 0.4-1.0 microns, that is, in visible light and beyond red into the invisible, longer wavelength near-infrared range [16].

The multicolor nature of *Galileo*'s images can reveal aspects of the geology of the lunar surface that are not discernable from monochromatic, black-and-white images. Only a handful of minerals compose nearly all of the rocks on the visible surface of the Moon. The highlands are dominated by light-colored, aluminum-rich minerals called feldspars, and the dark color of the mare plains results from mixture of iron- and magnesium-rich ("mafic") minerals with a smaller fraction of feldspar and a titanium-rich mineral called ilmenite. Each of these minerals has a subtly different color within the wavelength range visible to the SSI camera, so that the color of a particular rock provides information on its mineral makeup.

Actual samples of lunar rock and soil have been returned to Earth only from six *Apollo* landing sites and three sites visited by automated Soviet *Luna* spacecraft. Detailed compositional information has therefore been determined directly only for a very restricted set of areas, all on the near side. By using *Galileo* images and laboratory measurements of returned lunar samples, compositional information provided by color was extrapolated away from the landing sites into regions seen poorly or not at all from Earth, including the lunar far side [17,18]. This was accomplished by a two-step procedure. First, to enhance the very subtle color differences on the lunar surface, images acquired through filters showing important color contrasts were ratioed to each other. Second, the image products were calibrated to the landing sites. Returned rocks and soils from the landing sites, whose color properties were measured in the laboratory, serve the same role as human flesh does when a color television is adjusted: by "tuning" color to accurately represent these known areas, an accurate color of unknown areas simultaneously results. These color determinations, when compared to color and compositional measurements of the returned samples, provide information on composition in areas from which samples have <u>not</u> been returned.

For example, the ratio of brightness in the 0.40 micron "violet" filter to brightness in the 0.75 micron filter is particularly useful geologically. Higher ratios indicate a "bluer" soil - in other words, a soil that reflects relatively more light at short wavelengths such as blue. In well-developed mare soils returned to Earth, a very "blue" soil color has been found to indicate a basalt composition rich in titanium. Maps of the near side constructed from ratioed telescopic photographs demonstrate a variety of mare units with different "bluenesses," and thus contents of titanium [19]. *Galileo* images yield analogous information on basalt compositions, except that they show not only the near side but also far side regions invisible from Earth [20]. Similarly, mafic minerals in returned lunar samples strongly absorb near-infrared light with a wavelength of about 1.0 micron, whereas feldspars do not. The ratio of brightness in the 1.0 micron SSI filter to brightness in the 0.75 micron filter is thus a measure of the content of mafic minerals in surface materials. This procedure of extrapolating compositional information into areas not sampled by landers has allowed us to determine some of the basic compositional properties of Orientale and other far side basins.

The landscape and physical geology of the Orientale basin are known from photographs acquired during American *Lunar Orbiter* and *Apollo* missions and by Soviet *Zond* spacecraft [3,8,10,11,12,13]. The basin's topographic depression is bounded by the 900-km diameter Montes Cordillera ring, which consists partly of an inward-facing scarp and partly of high

mountains. Two inner concentric rings of high mountains, 480 and 620 km in diameter, are known collectively as Montes Rook. Outside of Montes Cordillera lies a broad region of ridges and grooves generally arranged radially to the basin. This surface, known geologically as the "Hevelius Formation," is interpreted as ejecta thrown from Orientale at the time of the basin-forming impact. The surface between Montes Cordillera and Montes Rook, the "Montes Rook Formation," is characterized by roughly equidimensional knobs 2 to 5 kilometers across set in smooth to gently rolling surface terrain. This origin of this material is not so well understood; some planetary scientists believe that it is also ejecta lofted by the basin-forming impact, but derived from deeper in the Moon than the Hevelius Formation. Light-colored plains inside the Montes Rook rings, the "Maunder Formation," have a cracked surface suggestive of cooling and fracturing of highland crustal material melted by the heat of the basin-forming impact. Three small regions of mare, Mare Orientale at the center of the basin and Lacus Veris and Lacus Autumnii nestled between the basin rings, account for the very limited amount of younger mare basalts erupted here. Very little is known about composition of the materials forming the basin: spectroscopic studies from Earth, where Orientale is barely visible, do indicate a feldspar-rich composition poor in mafic minerals [21].

Multicolor *Galileo* images of the Orientale basin have provided new indications of the composition of these geologic formations, so that questions about the origin and evolution of lunar basins can be more fully addressed [22]. Overall, like typical feldspar-rich highlands, the basin interior has a low abundance of mafic minerals indicating that basin formation did not excavate radically different rock types from depth. However one large crater within the Montes Rook Formation, called Lowell, does have an enhanced content of mafic minerals. The lunar mantle and lower crust are thought to be richer in mafic minerals than the upper crust forming the typical highlands, so Lowell may be a site where deep-seated rocks uplifted by basin formation have been exposed. The Maunder Formation and Montes Rook Formation appear as annuli with distinctive color properties, suggestive perhaps of small variations in feldspar-rich rock compositions. The Hevelius Formation exhibits subtle, patchy color variations, but there is no evidence of a concentric compositional zonation that might have resulted if the basin formed in a compositionally layered crust.

In the southeastern part of the Hevelius Formation, both the Hevelius Formation itself and small craters formed on top of it show evidence for a greater abundance of mafic minerals than in the basin interior or in typical highlands. The enhanced-mafic region covers an area of 200,000 to 400,000 square kilometers, comparable to the size of some of the smaller maria. The region also contains craters with dark haloes, seen from Earth and thought to have formed by excavation of a dark layer of mare material from a shallow depth [23,24]. This evidence all points to the existence of very old mare plains, buried by the Hevelius Formation when it formed as ejecta from the Orientale basin, whose ancient lavas have been excavated by small craters penetrating the thin ejecta layer. The presence of this mantled mare or "cryptomare" substantiates evidence from other studies which suggests that mare volcanism began before the end of the period of formation of large basins [25].

Galileo images of the lunar far side highlands also show the region of the South Pole-Aitken basin, one of the oldest known large basins on the Moon. With a diameter of 2000 kilometers, it is also the largest well-documented lunar basin [26]. Compared to typical highlands, the interior of the South Pole-Aitken basin is darker-colored in monochromatic images taken through single filters, though not as dark as the mafic-rich mare lavas. Multicolor images show that the content of mafic minerals within the basin is greater than in surrounding highlands, and the mafic content varies across the basin floor. Some mare plains occur here as scattered small patches [20,26], but are too small to account by themselves for the relatively large mafic component throughout the basin interior. Measurement of gamma-rays from the lunar surface, taken during the *Apollo* missions, also show that highland material within the South Pole-Aitken basin has a larger iron content than do typical highlands [27]. These observations present a contrast with the smaller

Orientale basin, where there is little evidence of magnesium- and iron-rich mafic rocks forming the basin's interior. Based on this combination of data from *Apollo* missions and *Galileo*, it appears that the South Pole-Aitken basin either contains a cryptomare or excavated mafic-rich rocks from the lower crust or upper mantle.

In summary, multicolor images of the Moon obtained by *Galileo* reveal variations in color properties of the lunar surface. Using returned lunar samples as a key, the color differences can be interpreted in terms of variations in the mineral makeup of the lunar rocks and soil. Thus the combined results of *Apollo* landings and multicolor images from *Galileo* allow extrapolation of surface composition to areas distant from the landing sites, including the far side invisible from Earth. Two very large impact basins visible in the multicolor images of the far side, the Orientale and South-Pole Aitken basins, have very different compositional properties as shown by these images. The Orientale basin, with a diameter of 1200 kilometers, appears to have excavated into rocks very similar to typical lunar highlands, rich in feldspars and poor in mafic minerals. Ejecta thrown out of the basin during its formation apparently thinly covered a substantial region of very old mare to the southeast, but the mare's dark mafic rocks have been excavated by later impact craters. In contrast, the interior of the 2000-km diameter South Pole-Aitken basin is much richer in mafic minerals than the surrounding highlands. Perhaps the South Pole-Aitken basin also contains regions of thinly covered ancient mare; alternatively, because it is larger that the Orientale basin, perhaps it excavated rocks richer in mafic minerals from the Moon's lower crust or upper mantle.

References. [1] Stuart-Alexander, D. and K. Howard, *Icarus*, *12*, 440-456, 1970. [2] Hartmann, W. and C. Wood, *The Moon*, *3*, 3-78, 1971. [3] Hartmann, W. and G. Kuiper, *Lunar and Planetary Laboratory Comm.*, *1*, 541-66, 1962. [4] Hartmann, W., *Icarus*, *17*, 707-713, 1972. [5] McCauley, J., *Am. Inst. Aeronautics Astronautics Jour.*, *6*, 1991-1996, 1968. [6] Gilbert, G., *Philosoph. Soc. Wash. Bull.*, *12*, 241-292, 1893. [7] Baldwin, R., Univ. of Chicago Press, Chicago, 1949. [8] Baldwin, R., Univ. of Chicago Press, Chicago, 1963. [9] Wilhelms, D. and J. McCauley, *U.S.G.S. Map I-703*, 1971. [10] Wilhelms, D., *U.S.G.S. Prof. Pap. 1348*, 1987. [11] McCauley, J., *U.S.G.S. Map I-491*, 1967. [12] McCauley, J., in *Mantles of the Earth and Terrestrial Planets*, edited by S. Runcorn, pp. 431-460, Interscience, New York, 1967. [13] Head, J., *The Moon*, *11*, 324-356, 1974. [14] Fanale, F., *EOS*, *71*, 1803, 1990. [15] Belton, M. *et al.*, *Lunar Planet. Sci. XXII*, in press, 1991. [16] Belton, M. *et al.*, *Space Sci. Rev.*, in press, 1991. [17] McEwen, A. *et al.*, *Lunar Planet. Sci. XXII*, in press, 1991. [18] Pieters, C. *et al.*, *Lunar Planet. Sci. XXII*, in press, 1991. [19] Pieters, C., *Proc. Lunar Planet. Sci. Conf. 9th*, 2825-2849, 1978. [20] Greeley, R. *et al.*, *Lunar Planet. Sci. XXII*, in press, 1991. [21] Spudis, P. *et al.*, *J. Geophys. Res.*, *89*, C197, 1984. [22] Head, J. *et al.*, *Lunar Planet. Sci. XXII*, in press, 1991. [23] Hawke, B. and J. Bell, *Proc. Lunar Planet. Sci. Conf. 12th*, 665, 1981. [24] Bell, J. and B. Hawke, *J. Geophys. Res.*, *89*, 6899, 1984. [25] Schultz, P. and P. Spudis, *Proc. Lunar Planet. Sci. Conf. 10th*, 2899, 1979. [26] Stuart-Alexander, D., U.S.G.S. Map I-1047, 1978. [27] Metzger, A. *et al.*, *Geochim. Cosmochim Acta*, *2*, 1067, 1974.

HUBBLE SPACE TELESCOPE OBSERVATIONS OF MARS; Philip B. James, University of Toledo, Toledo, OH; Todd Clancy and Steve Lee, LASP, University of Colorado, Boulder, CO; Ralph Kahn and Richard Zurek, Jet Propulsion Laboratory, Pasadena, CA; Leonard Martin, Lowell Observatory, Flagstaff, AZ; and Robert Singer, University of Arizona, Tucson, AZ.

Mars is relatively well known for an astronomical object having been visited by several spacecraft which have observed the planet from orbit and from the surface for a considerable length of time. Mars is like the earth in that it has an active atmosphere; the strong interactions between the atmosphere and surface of Mars make the planet quite variable in appearance on daily, seasonal, and interannual scales. So, despite the scrutiny of the red planet by spacecraft, more frequent, synoptic monitoring, such as that provided by terrestrial weather satellites, is needed to understand meteorology and air surface interactions on Mars.

Martian dust storms are a good example of such variable phenomena which are still only poorly understood. Small dust and sand storms were observed frequently on the martian surface by orbiting spacecraft, and both Mariner 9 and Viking witnessed a relatively rare global dust storm event in which dust spreads from growth centers in the southern hemisphere to cover essentially the entire planet. It is known that these spectacular events, which have no parallel elsewhere in the solar system, do not occur every (martian) year; and there is some evidence that their occurrence is variable on even longer timescales. Because of the effects that such events could have on manned or unmanned surface mission to Mars, the ability to understand and forecast these events is a highly desirable companion to renewed exploration.

The best record for studying the occurrence of duststorms and other variable phenomena has come from earth based astronomy. However, because the distance to Mars from Earth varies dramatically with time, the earth based record has been confined to times near oppositions, which occur every 26 months, when Mars is closest to Earth and can be studied in detail. For most of its orbital journey around the sun the angular size of Mars is too small for studying the planet from Earth. As a result, the available data on dust storms and other time variable phenomena are modulated by the opposition cycle, and a given season can only be viewed every fifteen years.

As originally designed, Hubble Space Telescope afforded the possibility of resolving features as small as 100 kilometers on the martian surface even when it is at the far point of its orbit; this is actually better than the resolution which can generally be obtained from Earth during the opposition periods. And, at oppositions, much better resolutions of roughly 20-30 kilometers, comparable to the set of Viking approach pictures,

would be possible. Hubble Space Telescope is therefore ideally suited for monitoring seasonal changes on the red planet. In practice, HST observations are constrained by the pointing constraint which prohibits pointing the telescope within 50^0 of the sun; for Mars, the period of possible observation is reduced to slightly over one half of the 687 day martian year.

This current project on Hubble Space Telescope was originally approved for a period of three years, commencing in late November of 1990 which coincided with a martian opposition. The seven scientists involved in this project have all been extensively involved in research related to variable features in the atmosphere and on the surface of Mars. The objectives of the proposed research include, in addition to study of martian dust storms: use of images obtained through different filters to study the spectral reflectance of regions on the martian surface in order to identify regional differences in surface composition and to record changes in surface "color" which have occurred since the Viking approach maps produced in the mid-Seventies; use of ultraviolet images obtained with the Planetary Camera and ultraviolet spectra obtained with the Faint Object Spectrograph to measure the amount of ozone in the planet's atmosphere as a function of location on the planet and to deduce the humidity of the atmosphere of Mars, which controls the amount of ozone; use of images to study changes in the albedo (relative reflectance) of the surface of Mars which are related to the movement and deposition of dust by the atmosphere; and use of Planetary Camera images to study martian clouds and to measure the opacity of the atmosphere. These goals were to be achieved using roughly monthly sequences designed to monitor the planet. In some cases, especially near the oppositions, several frequency filters were used to permit monitoring of color changes; when the angular size of the planet is smaller, red and blue filters will be used to discriminate between surface details, which stand out most in red, and atmospheric phenomena, which appear brighter in blue.

The General Observer Program of Hubble Space Telescope was postponed to provide the time required to deal with the various difficulties encountered by HST after launch. However, because of the time sensitive nature of the Mars observations (the 1990 opposition was in late November, and the next opposition, which is in January, 1993, will not be nearly as good), the Director approved the execution of the GO program as proposed. This program is therefore the first approved GO program to be executed. Experience with WFPC images of Saturn which were acquired in the fall led to the expectation that much of the resolution degradation caused by the spherical aberration present in the Hubble optical system could be eliminated through various deconvolution techniques. The Mars images, because of the large number of pixels and because of the complex surface details, presented a challenge to the deconvolution process, though the large signal to noise ratio possible for the bright target presented by Mars was a definite advantage. The Richardson-Lucy

technique has been used on the WFPC images of Mars; though the estimation of surface resolution is somewhat subjective, we estimate that this deconvolution technique has restored the resolution to within approximately a factor of two of that originally anticipated.

The images which have so far been reduced and analyzed show the face of Mars which features some of the most prominent surface markings on the planet. The largest dark albedo feature, Syrtis Major, was originally recognized by Huygens in the Seventeenth Century; it was used to derive the roughly 24 hour 40 minute rotation period of the planet. Syrtis is located on a large, regional slope from Arabia on the west to the Isidis Basin on the east; the low albedo of the region may be due to scouring of bright dust from its surface by regional winds. The bright feature to the south of Syrtis is the Hellas basin. This feature is the remnant of a huge impact on the planet roughly three and one half billion years ago which produced a basin roughly 800 kilometers in diameter and as much as four kilometers in depth. This basin is often seen to be heavily clouded or to have its surface covered with frost; at this date in late summer, its surface is uncharacteristically visible. Hellas is often the source for planetary dust storms, although none were identified in these images. The bright area to the west of Syrtis major is Arabia, which is elevated above the volcanic plains which surround it; the high albedo of Arabia and other bright areas is thought to be the result of a thin layer of dust deposited on the surface. Because of the prominent surface markings and because the region is known to generate many duststorms, this face of the planet will be monitored fairly continuously during the observing program.

Another feature in the images which attracts immediate notice is the bright, bluish north polar hood. This cloud canopy generally covers the north polar cap of Mars during fall and winter. It is meteorologically one of the most active regions of Mars; the periphery of the hood is characterized by baroclinic weather systems which are similar in structure to those found in terrestrial mid-latitudes. Details seen in the images suggest that such structures can be monitored using HST sequences. The clouds in the south may be the harbinger of a similar hood in the south. This season is particularly difficult to image from earth, and the existence of a south polar hood is controversial. HST images will be able to resolve this question.

Analyses of the data obtained so far are very preliminary because most of the time has been invested in calibration and deconvolution of the images. Preliminary examination of the images suggests that the data will allow the participating scientist to achieve the goals stated above. The first phase of the observing program has certainly reinforced the opinion, stated above, that Hubble Space Telescope is ideally suited to planetary observations.

EVIDENCE FOR AMMONIUM-BEARING MINERALS ON CERES; **T.V.V. King, R.N. Clark, W.M. Calvin, D.M. Sherman, G.A. Swayze (U.S. Geological Survey, Denver), and R.H.Brown (J.P.L., Pasadena)**

Evidence for ammonium-bearing minerals has been found on the surface of the largest asteroid Ceres. This is the first direct evidence for the occurrence of ammoniated-minerals on any planetary body besides the Earth. The presence of ammonium-bearing clays suggests that Ceres has experienced a period of alteration by substantial amounts of an ammonium-bearing fluid. The presence of the ammonium-bearing clays does not preclude Ceres maintaining a volatile inventory in the core or in an volatile-rich zone at some distance below the surface. Recent telescopic observations of Ceres, using the 3.0 meter NASA Infrared telescope facility on Mauna Kea have prompted this reevaluation of its surface mineralogy.

The basis for this study is the use of infrared spectroscopy to make mineralogic identifications on the surface of Ceres using an Earth-based telescope. Spectral reflectance data measures the interaction of light with materials, in this case minerals. Reflectance spectra of minerals have been measured in the laboratory and supplemented with theoretical spectra to provide a library for comparison with telescopic data. Theoretical spectra are derived by applying mathematical formula that incorporate physical constants describing the behavior of various minerals. The interaction of sunlight or "white light" with minerals causes specific wavelengths of the light to be absorbed. The wavelengths absorbed, the intensity of the absorptions and the width of the absorptions are unique from mineral to mineral. The light reflected from each mineral has a characteristic spectrum of wavelengths. The advantage of a theoretical approach is that many more spectra can be derived compared to time-consuming laboratory measurements.

Reflectance data were collected from Ceres, an approximately spherical body with a diameter of 913 kilometers. These spectra were than compared to previously collected laboratory spectra and theoretically-derived spectra in order to identify specific minerals on the surface of Ceres.

Our recent telescopic observations of Ceres indicate an absorption feature at 3.07 μm which we attribute to the presence of ammonium-bearing minerals. This absorption feature was first reported by Lebofsky et al. (1) to occur at 3.07 μm and was believed to be result from the presence of water-ice on the surface of Ceres. However, the wavelength position and the width of the absorption feature on Ceres are very similar to the absorptions resulting from the presence of the ammonium ion in clay minerals.

The spectrum of Ceres was compared to laboratory prepared and naturally occurring clays containing ammonium to determine the best spectral match. Several different structural and chemical types of clays were treated with ammonium chloride. The ammonium-chloride solution interacts with the clay minerals and replaces ions within the clay structure with the ammonium ions. Of the several types of clays tested, the best spectral match for Ceres was an ammonium-bearing saponite. Saponite is a clay mineral which is commonly found on the Earth and commonly forms when basic rocks are altered by hot fluid Weaver and Polland (2). Saponite is also found as an aqueous alteration product in carbonaceous chondrite meteorites Zolensky and McSween (3); and

references therein).

Comparison of the laboratory spectra and our Ceres data indicate that the ammonium absorption feature on Ceres is centered at 3.07±0.02 μm vs. 3.05 μm for the ammoniated-saponite. The width of the Ceres absorption feature is 0.113±.08 μm vs 0.145 μm for the laboratory sample. The depth of the 3.07 μm feature on Ceres is approximately 8 %.

Previous studies of Ceres have attributed the absorption feature at 3.1 μm to the presence of water-ice. However, theoretical calculations of the water-ice using many different grain sizes are not in accord with this interpretation. For instance, the water-ice at 1 and 0.3 μm grain sizes produces an absorption that is too wide and centered at too long a wavelength to be a good match for the Ceres spectrum.

To help us better understand what materials and how much of each material is necessary to produce Ceres spectrum, we completed two important studies. Firstly, we derived theoretically spectra involving mixtures of three components. Secondly, we measured laboratory spectra of three-component mixtures. We computed a spectrum which had nearly the same brightness and an absorption feature at 3.07 μm which was comparable in strength to that seen in the Ceres spectrum. The mixture simulated the ammonium-bearing clay and included two non-specific minerals to provide dark and medium color. On Ceres we might expect these materials to be a carbon compound and mafic silicates, respectively. We also calculated a spectrum in the same proportions as above, substituting water-ice for the ammonium-bearing clay. The resulting spectra produced an absorption feature which was dominated by a very broad water-ice absorption and does not resemble the spectra of Ceres. Thus, both theoretical and laboratory studies confirm that an ammonium-bearing phase, not water-ice, is an essential component of the Ceres spectra.

Assuming that the asteroid Ceres contains primitive material, then non-equilibrium or equilibrium condensation of the solar nebula could incorporate ammonia into Ceres (Lewis and Prinn (4)). During non-homogeneous accretion, ammonium salts and ammonia-ices condense below -70 C and thus would be incorporated into the outer shell of an accreting object. Equilibrium accretion models assume a solar nebula having solar elemental composition and examine the types of minerals that condense as the nebula cools below ~1350 C. As expected, refractory oxides condense first but water ices and hydrates (water ices with various trapped gases) do not condense until the nebula cools below 30 C.

In a series of papers, John Lewis and co-workers have demonstrated that only limited amounts of ammonia (NH_3) and methane (CH_4) can be produced during nebula cooling. Importantly, at temperatures near -80 C, when water ice condenses, ammonium bicarbonate and ammonium carmate may also condense. Thus, the potential exists for incorporating ammonium-bearing materials into accreting bodies in the late stage of their growth.

Thus, a body of theoretical evidence predicts that ammonium-bearing phases may be incorporated into the solar system bodies at low temperatures. The question then arises, how does the observation of ammonium-bearing saponite (a clay) fit into this picture ? Hydration of anhydrous nebula minerals, to produce clays, within the nebula cannot occur at temperatures above 30-80 C

and hydration reactions are very slow. Thus, it seems unlikely that ammoniated-saponite is a primary nebula mineral. A secondary alteration process seems a more likely explanation. Internal heating of Ceres, at temperatures approaching 130 C, may generate fluids enriched in ammonia and other ions, which react with anhydrous silicates to produce secondary clays. The results of such fluid interactions are observed in the carbonaceous chondrites and can be postulated for the Ceres.

(1) Lebofsky, L.A., M.A. Feierberg, A.T. Tokunaga, H.P. Larson, and J.R. Johnson, 1980, *Icarus*, 48, Scientific, 213p. (3) Zolensky, M. and H.Y. McSween, 1988, University of Arizona Press, 114-143. (4) Lewis, J.S. and R.G. Prinn, Academic Press, 470p.

TRITON: A HOT POTATO?; R. L. KIRK*, AND R. H. BROWN†, *U.S. Geological Survey, Flagstaff, AZ 86001, †Jet Propulsion Laboratory, Pasadena, CA 91109

Introduction Since the 1989 flyby of Triton by Voyager 2, considerable attention has been given to the effect of sunlight on the surface of that body: widely disparate models of the active geysers observed by Voyager have been proposed by us and by others, with a solar energy source almost their only common feature; other workers have struggled to explain the seemingly paradoxical distribution of surface frost, with an extensive polar cap in the hemisphere currently most heated by the sun but no visible cap in the less-illuminated northern hemisphere. Yet Triton derives more of its heat from internal sources than any other icy satellite, and perhaps more than any other solid body in the solar system except Io. On the one hand, Triton is located 30 times as farther from the sun than the Earth is, and reflects away the majority of the solar radiation incident upon it. On the other, the high bulk density of Triton indicates that rock substantially outweighs ice in its makeup, so that energy released by the decay of radioactive elements is correspondingly more important for Triton than for other icy satellites. We have begun to investigate how this relatively large internal heat source might affect the observable behavior of volatiles on Triton's surface.

The Global Energy Budget How much energy is liberated by the decay of radioisotopes in Triton's interior, and how much does the satellite receive on average from the sun? One of us (Brown) and coworkers have tried to answer these questions in a paper recently submitted to *Science*. Both quantities turn out to be uncertain by about a factor of two. The internal heat flux could be as low as $3.3\,mW\,m^{-2}$ or as high as $6.6\,mW\,m^{-2}$, depending mainly on whether the rock in Triton has a composition more like that of chondritic meteorites or like that of the Moon. (For comparison, the Earth's internal heat flow is roughly $60\,mW\,m^{-2}$.) The incident solar energy is much greater, at $1.5\,W\,m^2$, but only a fraction is absorbed (roughly one fifth by past estimates, but perhaps as little as one tenth according to Brown and coworkers), and, of course, only a part of the surface is illuminated at any time. The absorbed solar energy, averaged over the whole surface, is probably between 40 and $80\,mW\,m^{-2}$. Internal heat thus amounts to somewhere between about 5% and 20% of Triton's global energy supply.

Inclusion of a spatially uniform internal heat supply in Triton's energy budget would not have any observable effect on surface frosts (although it would imply that, in order to maintain the surface temperature measured by Voyager, Triton's surface must radiate heat slightly more efficiently than previously thought). If the internal heat flux is spatially variable, however, frost stability will be enhanced in areas of low heat flux and decreased in areas of high flux. The relatively large *average* internal energy supply encouraged us to

TRITON'S INTERNAL HEAT: R. L. Kirk and R. H. Brown

try to estimate the magnitude of internal heat flux *variations* and to evaluate their potential effect on the distribution of surface volatiles. We have considered the insulating effect of the polar caps, the nonuniform heat flow due to mantle convection, and the localized heating due to cryovolcanic activity.

Insulating Polar Caps We are ultimately interested in the effect of internal heat on the distribution of surface volatiles. The distribution of volatiles may, however, significantly influence the internal heat flux. The thermal conductivity of solid nitrogen at Triton temperatures is several hundred times less than that of water ice. A polar cap on the order of a kilometer thick may thus have an insulating effect comparable to the entire icy outer layer of Triton, which is probably about 350 km thick. We have constructed a simple analytic model to test this effect, assuming thermal conduction in a spherical shell (the thermal lithosphere) with a constant temperature maintained by the convecting ice mantle at its base and an insulating cap whose thickness varies smoothly with latitude from zero at the equator to a maximum at the poles. We find that for a nitrogen cap 1 km deep, the equatorial heat flux can be increased to as much as 1.4 times the global average, while the flux at the poles is reduced to only 0.3 of the average value in the extreme case.

Effect on Frost Stability Published models of the current energy balance on Triton (excluding internal heat but including the variation of albedo with latitude) predict the deposition of frost northward of 15° latitude; time-dependent models predict that seasonal frost deposits currently extend even farther south. Can we account for the absence of obvious bright frost deposits in Triton's northern hemisphere by including the concentration of internal heat toward the equator in the energy balance? The answer would appear to be no. We have performed a frost stability analysis similar to that by John Stansberry of the University of Arizona and coworkers. Adding a spatially varying internal heat flux shifts the current latitude of frost deposition by no more than 0°.5.

Somewhat less can be said with certainty about the effect of internal heat on the long-term stability of the polar caps. The seasonally averaged insolation varies much less strongly with latitude than the current diurnally averaged insolation, so that addition of internal heat should have a proportionally larger effect on frost stability. By an unfortunate coincidence, however, the seasonally averaged insolation curve has almost exactly the same shape as our simple model for the redistribution of heat by the polar cap. Including internal heat in our calculation thus has the same effect as would increasing the brightness of the sun: the latitude dividing long-term net sublimation from net deposition does not shift, although the rates of sublimation and deposition are increased. We are presently working on a numerical model that will incorporate more general cap thickness profiles (including an

unfrosted equatorial zone that does not participate in the energy balance of the caps) and that will follow through time the feedback between cap thickness and the redistribution of internal heat. This feedback mechanism may well be an important (and previously overlooked) piece of the puzzle that is Triton's global frost distribution.

Mantle Convection We turn now to processes capable of producing more localized enhancement of heat flux and thus perhaps able to modify the pattern of frost deposition. One candidate is mantle convection: upward heat flux at the top of the mantle is concentrated over zones of upwelling. Lateral heat conduction in the thermal lithosphere will, however, act to smooth out or attenuate the variation in heat flux. We have modeled this attenuation, which depends on the thickness of the lithosphere, the horizontal scale of mantle convective cells (proportional to mantle thickness) and the planform of convection (one-dimensional rolls *versus* polygonal cells). For roll convection and our upper limit on average heat flux the variation in surface flux would be sufficient to shift the latitude of frost equilibrium by $\pm 2°$. If the mean flux is smaller, the variable portion will be much more strongly attenuated, resulting in a neglibable effect. We conclude that it is barely possible that mantle convection modulates the shape of the polar cap edges in an observable way.

Cryovolcanism Many of the surface features revealed by Voyager 2 on Triton have been interpreted as evidence of "cryovolcanism," that is, geologic activity analogous to volcanic eruption on the terrestrial planets but involving ices such as H_2O, NH_3, CH_4, or N_2 and occurring at much lower (though well above ambient) temperatures. Unlike the mechanisms discussed above, migration of "hot" cryovolcanic material toward or to the surface of Triton could result in heat fluxes that exceed the global average by a large factor. On the other hand, this enhancement would be transient and hence might not be observed at a given time. We have considered the possible effects of two very different types of cryovolcanic activity.

Linear ridges a few hundred meters high, tens of kilometers wide, and thousands of kilometers long are common in Triton's cantaloupe terrain and extend into the southern polar cap. They have been interpreted as the result of fissure eruptions. We have modelled the thermal effect of the warm material in the conduit feeding such an eruption, and we find that temporary heat flux enhancements comparable to or greater than the global average flux would occur in a zone extending 17 km to either side of the dike and would last up to 10^5 years. This result leads us to speculate that the narrow swath apparently cleared through the polar cap margin by one of the linear ridges may result in part from heating by the surface flow and its conduit. The critical problem with this suggestion is the low probability (on the order of 1%) of Voyager observing a ridge soon enough after its eruption that the heatflow

TRITON'S INTERNAL HEAT: R. L. Kirk and R. H. Brown

is still enhanced. This difficulty might be overcome if openings in the permanent polar cap, once created, are able to persist for much longer than 10^5 years because the material exposed in this way is darker than the cap and absorbs enough more sunlight to remain significantly warmer.

We have also considered the thermal effects of diapirs: buoyant masses of warm ice or other cryomagma that are not confined to a conduit, but instead ascend through the lithosphere as roughly spherical "blobs." Because the viscosity of the lithospheric ice is very high (and increases dramatically with decreasing temperature) the diapirs propagate upward by softening and pushing aside a thin layer of the surrounding ice at the expense of their internal heat, in a kind of upside-down "China syndrome." Modeling this behavior, we find that a diapir typically ascends 1.0–1.5 of its own radii before running out of heat. The enhancement of surface heat flux depends on the depth at which the diapir stops; a diapir 70 to 100 km in radius will ascend far enough to double the heat flux in the region above it. The flux enhancement will last on the order of 50 to 100 million years, so that observation of the thermally active phase is far more probable than was the case for the linear ridges. We suggest that the three diffuse, roughly circular regions of lower albedo at latitude 5° S, longitudes 25°–50° on Triton may be the result of sublimation of the surface frost by diapiric activity. The features are roughly 50 km in radius, and at least two of them are clearly associated with cryovolcanic flooding of the surface. They may therefore constitute the clearest evidence for the modification of Triton's frost layer by localized internal heating.

STABLE HYDROGEN AND CARBON ISOTOPE RATIOS OF EXTRACTABLE HYDROCARBONS IN THE MURCHISON METEORITE; R.V. Krishnamurthy and S. Epstein, Division of Geological & Planetary Sciences, Caltech, Pasadena, CA 91125, S. Pizzarello, J.R. Cronin and G.U. Yuen, Department of Chemistry and Center for Meteorite Studies, Arizona State University, Tempe, AZ 85287.

Researchers have been engaged for several decades in the study of meteorites, one of the most primitive materials in the solar system, to unravel the mysteries that shroud the origin of the solar system. Detection of organic compounds in a variety of meteorites has opened up new possibilities to look for fresh clues in the cosmochemistry. Evidence for the presence of such important compounds as amino acids, carboxylic acids and hydrocarbons are of particular interest in this context. Recent advances in analytical techniques have made it possible to extract and identify the minute levels at which these compounds exist in the meteorites. As is inevitable in the analysis of such low-level concentrations, these studies have generated some controversy regarding contamination. In simpler terms, the first step is to ensure that the compounds isolated from the meteorites are truly part of the meteorites and are not an artifact introduced by exposure to the terrestrial environment, storage or handling. Previous efforts to answer this question had met with only partial success. In a novel and fairly fool-proof method we have recently addressed this question with a greater degree of success.

We have measured the stable carbon and hydrogen isotope ratios in several of the chemical compounds extracted from the Murchison meteorite that fell in Australia in 1969. The results obtained by us in the study of amino acids in this meteorite gave very unusual hydrogen and carbon isotope ratios. We have now extended the technique to the different classes of hydrocarbons (compounds in which hydrogen atoms are attached to carbon atoms as for example methane). The hydrocarbons were isolated using a variety of separation techniques. As with the amino acids, the method involved the measurement of the ratio of deuterium to hydrogen and carbon-13 to carbon-12, the stable isotopic forms of the elements hydrogen and carbon respectively. Isotopes of different elements have similar chemical properties for all practical purposes except that they differ in their atomic weight. For instance, deuterium has an atomic weight of 2 compared to hydrogen's 1. Geochemists have known for a long time that ,despite their identical chemical properties, isotopes do behave somewhat differently during various physical and chemical processes that take place in nature. This behavior or fractionation is a very small effect but measurable to a high precision using modern mass-spectrometers. As an example, when water which is made up of hydrogen and oxygen atoms evaporates from the oceans or lakes the vapor phase is less enriched in deuterium and O-18(the heavier isotope of oxygen). During condensation of the vapor back into liquid water as in the form of rain, the reverse takes place with deuterium and O-18 concentrating in the liquid phase. Similarly, one of the most important processes in nature namely photosynthesis results in the plants preferentially utilizing C-12, the lighter isotope of carbon so that all plant material found in nature, living or dead, reflects this characteristics. As a general rule, the end product of all the biologic processes taking place on the earth are seen to be enriched in the lighter isotopes of carbon and hydrogen. The end product may be the various molecules synthesized by plants or animals when they are alive or those generated by the geochemical and geophysical alteration of living things.

Our isotopic investigation showed that several of the hydrocarbons isolated from the Murchison meteorite have higher deuterium to hydrogen ratios, most unlike that for any similar compounds found on the earth. Such an enrichment in deuterium in these compounds provides the first compelling evidence that they are a part of the meteorite and are not introduced from any terrestrial source. Simultaneous measurement of the stable carbon isotope ratio of the hydrocarbons also showed a concomitant enrichment in the heavier isotope, although to a lesser

degree than that of deuterium.

The above findings have great significance as to the origin of these organic molecules, because several of these compounds such as aldehydes, ketones, alcohols etc have also been observed in the dense interstellar cloud. This would support the contention that these compounds themselves or the basic units that make them up were created outside of the solar system somewhere in the interstellar space. It may be also recalled that astronomers have provided evidence for the existence of simple organic molecules in the interstellar space although evidence for higher order molecules such as amino acids has thus far been elusive. Since the cold reaches of the interstellar space appear to be much less conducive to chemical reactions that could produce viable compounds such as amino acids and hydrocarbons, special types of reactions known as ion-molecule reactions are thought to be a likely means of carrying out the necessary chemistry. One of the interesting observations to be made is that these hydrocarbons, as with the amino acids analyzed in the Murchison meteorite previously, have survived severe alterations since their formation. If not, they would have acquired the hydrogen isotope imprint of cosmic hydrogen or that in the dominant fraction of the meteorite matrix, both of which show no unusual deuterium enrichment. To strike a note of caution, our knowledge regarding the synthesis and incorporation of the various chemical entities in the Murchison or other meteorites is far from complete, but the detection of an unusual isotopic identity is a major step towards achieving that goal.

RELATIVE CHRONOLOGY OF MARTIAN VOLCANOES. R. Landheim[1] and N.G. Barlow[2], [1]Dept. of Geology, Louisiana Tech University, Ruston, LA 71272, [2]SN21, NASA/Johnson Space Center, Houston, TX 77058.

Impact cratering is one of the major geological processes that has affected the martian surface throughout the planet's history. The frequency of craters within particular size ranges provides information about the formation ages and obliterative episodes of martian geologic units. The Crater Analysis Techniques Working Group (1) recommended that crater size versus crater frequency data be graphically displayed using either the cumulative or relative plotting techniques. We choose here to use the relative technique because it more clearly displays frequency variations within a particular size range than does the cumulative technique. Two distinct curves result from the crater size-frequency distribution analysis of martian terrain units: lightly cratered regions show a flat curve on the relative plot and heavily cratered regions show a multisloped shape (Fig. 1). The transition between these two curves occurs near a log R value of -2. It is believed that these curves describe the population of impacting objects responsible for the cratering record at a particular period of time. Thus, based on the shapes of the crater size-frequency distribution curves, the impact cratering record of Mars can be divided into two distinct populations. The first population was emplaced during the period of high bombardment rates which existed in the inner solar system prior to about 3.8×10^9 years ago--this is the population which displays high crater density and a multi-sloped crater size-frequency distribution curve. The second population, characterized by a lower crater density and a flatter size-frequency distribution curve, has dominated the cratering record since the cessation of the heavy bombardment period (2).

In an earlier analysis, Barlow (3) used the relative plotting technique to revise the martian relative chronology based on craters ≥8 km in diameter. That study determined the relationship of twenty-three generalized geologic units to the period of heavy bombardment, based on the crater densities and shape of the size-frequency distribution curve of superposed craters. However, most martian volcanic constructs (because of their young ages or relatively small sizes) contain too few craters in this size range to make the results statistically reliable--thus crater analysis could not be used to include the volcanoes in the Barlow chronology. Other studies have included the volcanoes in both relative and absolute chronologies (4, 5, 6), but none of these analyses used the changing shape of the crater size-frequency distribution curves to determine the ages of features relative to the period of heavy bombardment.

This study extended the Barlow chronology by measuring small craters on the volcanoes and a number of "standard" terrain units. Inclusion of smaller craters in units previously analyzed by Barlow allowed for a more direct comparison between the size-frequency distribution data for volcanoes and established chronology. We mapped and identified 11,486 craters in the 1.5-8 km diameter range in selected regions of Mars, including portions of the heavily cratered intercrater plains of the southern hemisphere, the rim of the Isidis Basin, Syrtis Major, Lunae Planum, and various plains units in the northern hemisphere. Included in this study were the medium sized to large volcanoes in the Elysium (Elysium Mons, Albor Tholus, and Hecates Tholus), Tharsis (Olympus Mons, Ascraeus Mons, Arsia Mons, Pavonis Mons, Alba Patera, Biblis Patera, Ulysses Patera, Tharsis Tholus, Ceraunius Tholus, Jovis Tholus, and Uranius Tholus), and Hellas (Hadriaca Patera, Amphitrites Patera, and

Tyrrhena Patera) regions. The results of this study, summarized in Table I, give us a more precise estimate of the relative chronology of the martian volcanoes.

Most previous studies have generally determined that the highland patera (Hadriaca, Amphitrites, Tyrrhena, and Apollinaris Paterae) formed during a very brief episode extremely early in martian history, whereas the volcanoes in the Tharsis and Elysium regions are much younger (7). Our analyses suggest that some of the volcanoes in the Elysium and Tharsis regions are not as young (i.e., post-heavy bombardment age) as previously believed. These volcanoes include Albor Tholus, Ulysses Patera, Hecates Tholus, and Tharsis Tholus. Ceraunius Tholus, Jovis Tholus, and Uranius Tholus formed even earlier, during the early part of the heavy bombardment period. The highland patera are still found to be old (i.e., heavy bombardment aged), but are now seen to display a wider range of ages throughout the heavy bombardment period than previously believed.

The results of this study lend further support to the increasing evidence that volcanism has been a dominant geologic force throughout martian history (8). However, we must emphasize that all ages derived in this study are averaged over relatively large areas. Smaller regions within the areas studied are likely older or younger than the average age given here. Nevertheless, this technique reveals important new information about the relative ages of volcanic events on Mars.

Obliteration effects (erosion and/or deposition) manifest themselves in the cratering record as an abrupt decline in the frequency of craters less than a certain size. On the crater size-frequency distribution plots, this effect appears as a steep vertical drop at small crater diameters. Our analysis reveals several examples of likely obliteration episodes, as well as examples of recratering on a surface which underwent an obliteration episode in the past. These effects are factored into our age interpretation of the features studied in this project.

Continuing analysis of small impact phenomena will result in a more detailed understanding of martian geochronology. An extension of this research to other areas of Mars will broaden our understanding of how smaller areas fit into the chronology. It will also allow us to better define the extent and amount of obliteration that has occurred in various regions of the planet. Both of these topics will be of great importance in the scientific planning of future unmanned and manned Mars surface missions.

REFERENCES: (1) Crater Analysis Techniques Working Group (1978), *NASA Tech. Memo. 79730*, p. 1-20. (2) Strom R.G., Croft S.K., and Barlow N.G. (1991), in *Mars*, Univ. Az Press, in press. (3) Barlow N.G. (1988), *Icarus*, **75**, p. 285-305. (4) Neukum G. and Wise D.U. (1976), *Science*, **194**, p. 1381-1387. (5) Neukum G. and Hiller K. (1981), *J. Geophys. Res.*, **86**, p. 3097-3121. (6) Tanaka K.L (1986), *Proc. Lunar Planet. Sci. Conf. 17th*, p. E139-E158. (7) Carr M.H. (1981), *The Surface of Mars*, Yale Univ. Press. (8) Greeley R. and Spudis P.D. (1981), *Rev. Geophys. Space Phys.*, **19**, p. 13-41.

MARTIAN VOLCANO CHRONOLOGY: Landheim R. and Barlow N.G.

TABLE I
RELATIVE CHRONOLOGY OF MARTIAN VOLCANOES

Younger

Post Heavy Bombardment (Type Area: Northern Plains)
- Olympus Mons
- Pavonis Mons, Ascraeus Mons, Arsia Mons
- Alba Patera
- Elysium Mons, Biblis Patera

End of Heavy Bombardment (Type Area: Ridged Plains)
- Albor Tholus
- Ulysses Patera
- Hecates Tholus, Hadriaca Patera
- Amphitrites Patera

Heavy Bombardment (Type Area: Highland Intercrater Plains)
- Tyrrhena Patera, Tharsis Tholus, Apollinaris Patera
- Ceraunius Tholus
- Jovis Tholus
- Uranius Tholus

Older

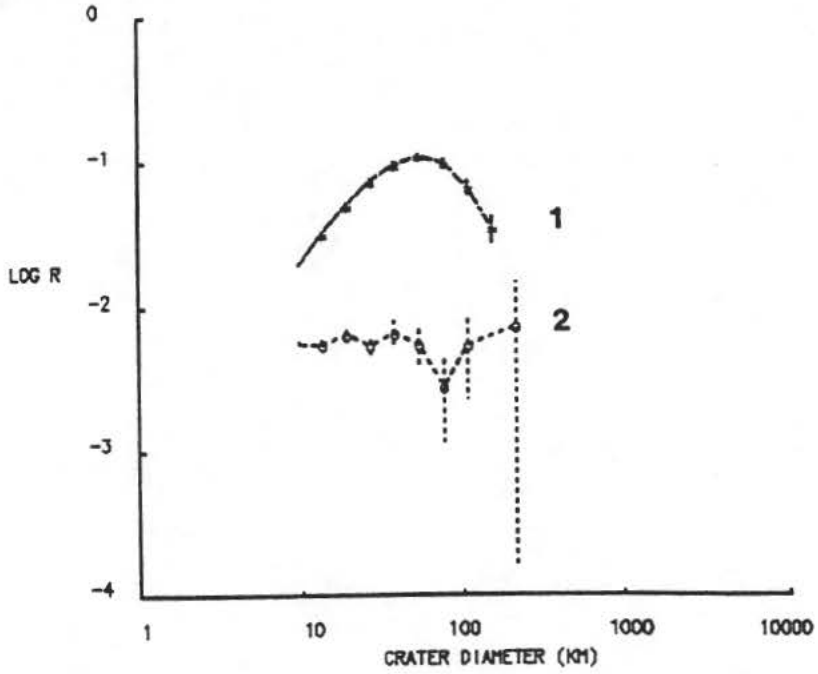

Figure 1: Crater size-frequency distribution plots for martian heavily cratered (1) and lightly cratered (2) regions, as displayed on a Relative Plot. The R value on the vertical axis is a parameter which normalizes the frequency of craters within a particular diameter range to a power law function of -2 slope. Surfaces whose crater size-frequency distribution follows this power law function will appear as a horizontal line on this graph. The difference in shape between the two curves is interpreted as reflective of differences in the size-frequency distribution of the impacting populations.

SPACE DEBRIS: ORBITAL MICROPARTICULATES IMPACTING LDEF EXPERIMENTS FAVOUR A NATURAL EXTRATERRESTRIAL ORIGIN

Professor Tony McDonnell

Unit for Space Sciences, Physics Laboratory, University of Kent at Canterbury, Canterbury, Kent CT2 7NR, United Kingdom

Telephone:
National (0227) 459616
International +44 227 459616

Keywords

Micrometeoroids, space debris, NASA Long Duration Exposure Facility, LDEF, hypervelocity impact, spacecraft damage.

Introduction

The results of work carried out at the Unit for Space Sciences at the University of Kent at Canterbury, United Kingdom, on the micrometeoroid and space debris environment of near Earth space are described in this article. The primary data for the research programme is supplied by an examination of several types of exposed surface from the NASA Long Duration Exposure Facility (LDEF) including an experiment dedicated to the detection of micrometeoroids and space debris provided by the University.

Extended Press Abstract

In the years leading up to the return of LDEF, work in examining retrieved surfaces from the repaired Solar Maximum Mission satellite had yielded the result that space debris was the most abundant component in the particle population in sizes ranging from 10^{-14} grammes (≈0.2 microns in diameter) to 10^{-9} grammes (≈9 microns diameter). A review of the interpretation of this data has cast doubts on that conclusion, and the examination of LDEF surfaces is beginning to provide a definitive answer both by trajectory analysis enabled by the attitude stabilisation of LDEF, and spectroscopy conducted at individual impact sites, yielding element and isotope chemistry.

The accompanying plot (figure 1) shows trends both in the number of Earth orbiting satellites and in the small particle population as observed by several spaceborne particle detection projects†. From this plot, there is no unambiguous indication that the small particle population encountered in low Earth orbit is in any way correlated with the satellite population (as would be the case with space debris) and seems to remain constant over a timescale of years; an expected characteristic of the natural interplanetary component.

Sufficient data will ultimately be derived from an examination of LDEF surfaces which will support or contradict this hypothesis on the basis of impactor chemistry; a generally unambiguous indicator of origin, extra-terrestrial or otherwise. Chemistry of impactor residues are derived from measurements made by X-ray and mass spectrometers at the University of Kent at Canterbury and elsewhere.

Good statistics have yet to be obtained from LDEF impact site chemical classifications; but the trend analysis presented above, and statistically sound flux data from several experiments plus analysis of engineering surfaces on LDEF,

---

† Note for Editors:

A simplification of this diagram would be to reproduce only the solid curve labelled 'Satellites' along with the three dotted curves labelled '5μm', '20μm' and '40μm'. These latter three should be re-labelled as 'greater than 2 picogrammes', 'greater than 130 picogrammes' and 'greater than 1000 picogrammes' respectively. These masses are those of the smallest particle that can perforate Aluminium foil of the given thickness at the typical velocities encountered in low Earth orbit (several kilometres per second or tens of thousands of miles per hour). A picogramme is one million millionth of a gramme or 28,375,000,000,000 to the ounce. A micron is one millionth of a metre, or 25,400 to the inch.

are beginning to indicate that an excess of natural small particles above the simple interplanetary mass distribution exists.Surprisingly, perhaps, these particles could be orbiting the Earth .

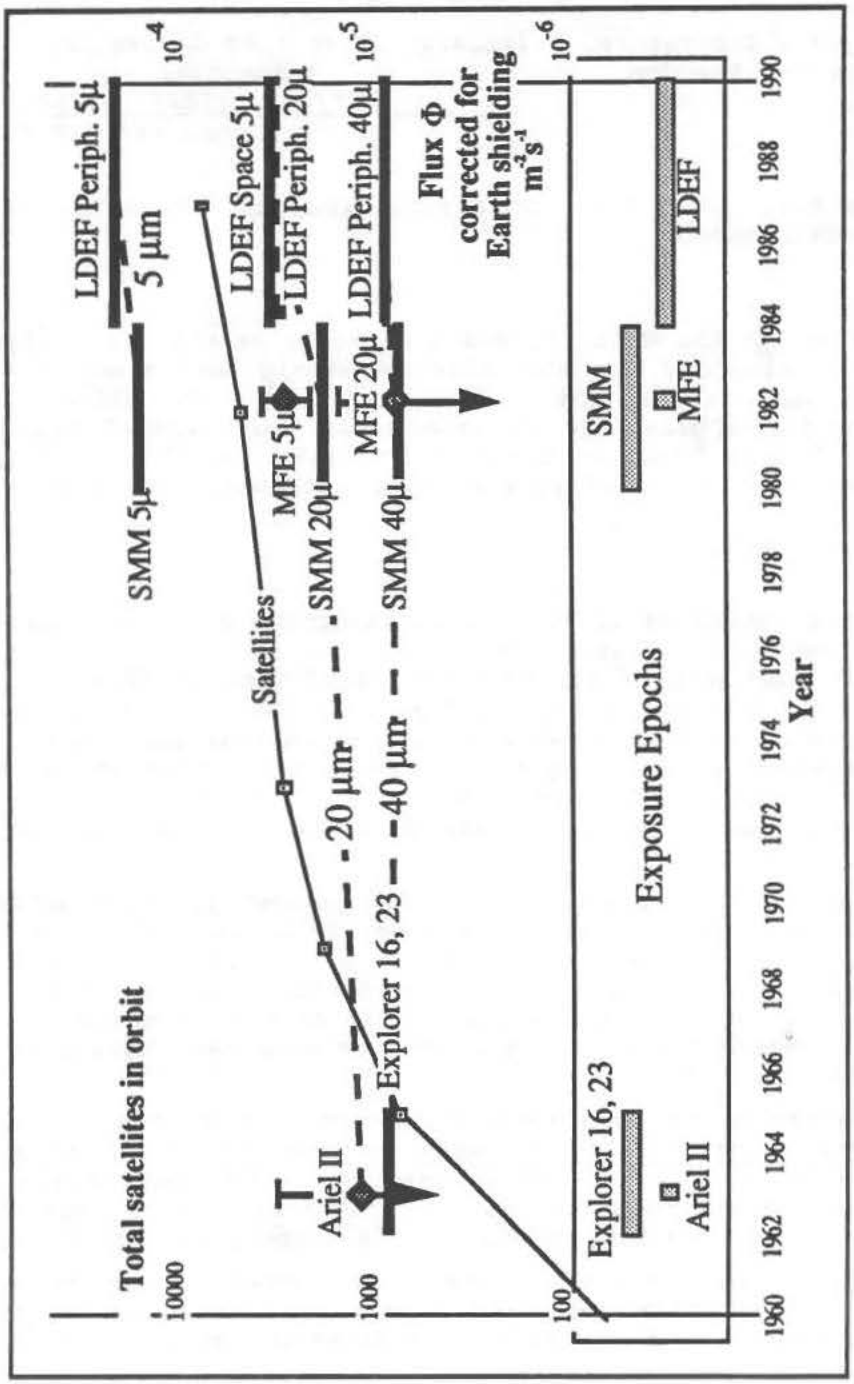

Figure 1. The long term evolution of the number of orbiting bodies in four size regimes; namely deliberately deployed satellites, and particles of such a size that they are capable of penetrating Aluminium foils of the three thicknesses. These latter three items of data, expressed as fluxes of particles per unit area per unit time, cumulative in size. The term cumulative in this context refers to the fact that each point represents all particles larger than the minimum size to achieve perforation.

This interim conclusion revives the once popular concept of a terrestrial dust belt, the origin of which is, as yet, unclear. Asteroidal and/or cometary sources are definite candidates, and the answer to this question may be derived from the chemistry of the debris found associated with impact sites. A description of the processes involved in this analysis follows.

Analytical techniques

In the range of particle sizes under discussion (micron scale), the damage experienced by spacecraft surfaces is in the form of minute craters (perforations in foils) of a characteristic form. This form invariably incorporates a lip or rim

around the crater, either continuous or made up of separate 'petals'. The profiles of craters, (the morphology) are symptomatic of 'hypervelocity' impact; that is an impactor velocity of greater than 3-4 kilometres per second. This distinguishing aspect allows the discrimination of damage caused on orbit from surface defects and other localised features. It is therefore important to image potential sites at high magnification, with a large depth of field; requirements which suggest the use of the Scanning Electron Microscope (SEM). This examination yields the size of the crater site, which by use of mathematical techniques verified in the laboratory over many years, yields the size of the impacting particle.

Conventionally, the SEM technique requires that the specimen be rendered electrically conducting by surface coating, but the University of Kent is equipped with an instrument whose performance allows operation in a regime where this is unnecessary. This latter is important where highly sensitive surface chemistry techniques are to be employed subsequent to the site location, classification and imaging stages in the analysis.

The first of these techniques is carried out in the SEM, by analysing the soft X-rays emitted by the specimen when the electron beam irradiates it. The energy distribution of these X-rays indicates the elements present in a thin layer on the order of a micron thick, and can be used to locate and identify areas of impactor debris deposits. These usually represent a very small fraction of the mass of the impactor, but some arrangements of target (the impacted surface) material, particularly thin foils, retain a significant proportion of impactor matter in a localised form. The University of Kent MicroAbrasion Package (MAP) experiment is just such an arrangement, and is thus a prime candidate to provide significant statistics on impactor chemical classes.

The most important classification in this context is that between space debris and natural micrometeoroids. While this was done with great success at impact sites on components of the Solar Maximum Mission satellite, chemical differences are not always clear cut. It is already known that major contributors to the micron sized debris population are Aluminium Oxide spherules, an effluent of upper stage solid rocket motor burns, and thermal control paint fragments whose chemistry includes Titanium Oxide. It is expected that many sites caused by impacts from such particles will be identified. Sites due to micrometeoroid impact, where impactor debris is extant, will have more complex chemistry, bearing some relation to the known compositions of stratospheric (Brownlee) cosmic dust particles and other extraterrestrial materials brought to Earth by various means.

Debris deposits, where the total amount is sufficient for the analyses, will be subjected to further techniques, notably mass spectroscopy which yields isotopic composition. This analysis can produce not only evidence of extraterrestrial origin but also detect the signature of an interstellar particle - that is material originating from a different stellar interior than that of the matter which formed our Solar System. The unambiguous identification of such an impactor has yet to be achieved from LDEF examination.

Epilogue

Data gathering on the low Earth orbit particle environment from LDEF surfaces continues apace at the University of Kent and elsewhere. In addition to the confirmation or contradiction of pre-LDEF conclusions on the composition of this population, much new information on the orbital distributions is emerging. The volume of potential data is such that some controversies will continue to rage for several more years, but already the puzzle has begun to unravel - aiding simultaneously the safe and efficient exploitation of near Earth space and our understanding of the origins of the Solar System. Technology driven needs such as the design of Space Station Freedom are looking to this LDEF data for design inputs on the hazards of this low Earth orbit particulate population.

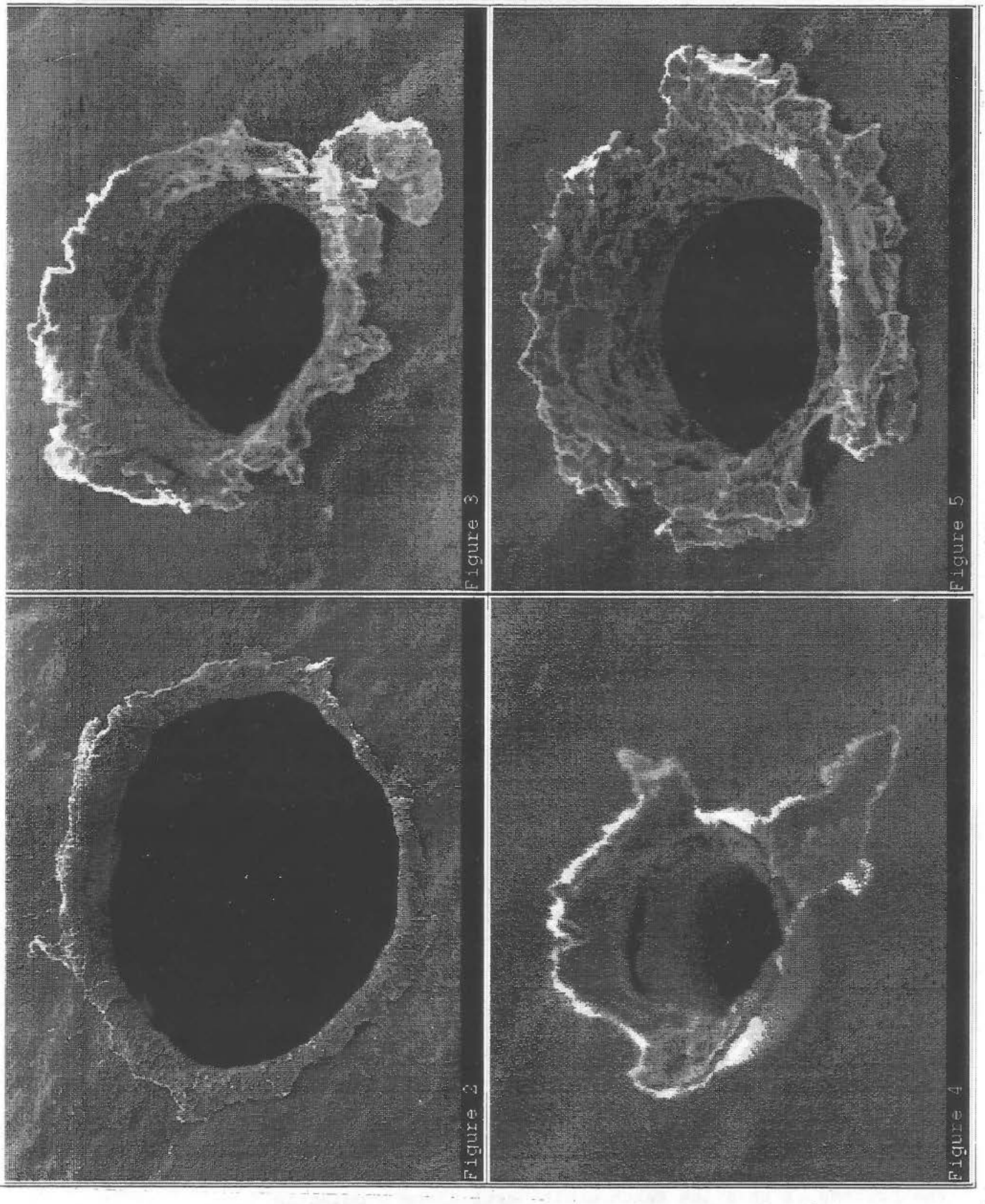

Caption for micrographs

Scanning Electron Microscopy images of hypervelocity impact craters puncturing the Canterbury MAP experiment. Though shown at high magnification, larger particulates could be expected to impact on Space Station Freedom and could penetrate its protective shield.

Experimental reduction of simulated lunar glass by carbon and hydrogen and implications for lunar base oxygen production.

David S. McKay and Richard. V. Morris
Solar System Exploration Division, NASA Johnson Space Center, Houston TX 77058

Amy J. Jurewicz
Lockheed Corp., Houston Tx 77058

Introduction: The most abundant element in lunar rocks and soils is oxygen which makes up approximately 45% by weight of typical lunar samples returned during the Apollo missions. This oxygen is not present as a gas but is tightly bound to other elements (mainly silicon, aluminum, iron, calcium, magnesium, and titanium) in minerals or glass. When people return to the moon to explore and live, the extraction of this oxygen at a lunar outpost may be a major goal during the early years of operation. It will likely be cheaper and more efficient to extract oxygen from local materials rather than bring it all the way up from earth, particularly when large quantities of oxygen are necessary. This oxygen will mainly be used for propellant to enable the lunar lander vehicle to go from the lunar surface to lunar orbit and return. It will also be used for life support and will likely be combined with extracted solar wind hydrogen to provide manufactured water to the outpost. In some scenarios, lunar-produced propellant would even be used to provide fuel for an expedition to Mars.

Because of the potentially large future cost savings which may come from the production of oxygen from local materials, it is very important to begin developing effective methods for extracting oxygen from lunar rocks and soil. Well over twenty different different chemical processes have been proposed for extracting oxygen from lunar materials. Only a few of these processes have had enough laboratory work performed to show that they really work. Among the most studied processes is the reduction of ilmenite by hydrogen gas to form metallic iron, titanium oxide, and oxygen. This process has recently been patented by Dr. Michael Gibson and Dr. Christian Knudsen of Carbotek, Inc. of Houston (patent number 4,948,477; August 14,1990). In this process, developed under NASA sponsorship, the hydrogen extracts the oxygen atoms bound to the iron in ilmenite. The patent also covers the reduction of lunar agglutinates which are small glass-bonded aggregates of lunar minerals formed by micrometeorite impacts. The hydrogen combines with the extracted oxygen to produce water which then removed from the reactor and electrolyzed. The oxygen can be collected and stored and the hydrogen can be recycled. The processing would take place in a fluidized bed reactor similar to those used in the chemical processing industry for many applications, including the processing of iron ore to extract iron metal. While this process has many advantages compared to some others, it also has some disadvantages. It requires an ilmenite-rich starting material, limiting the lunar site location to high-titanium mare regions. It requires that the ilmenite be concentrated by beneficiation methods, a process which is likely to be complex and possibly inefficient, particularly for mature lunar soils. Immature soils might permit easier concentration of ilmenite, but such soils may be much less abundant on the lunar surface than mature soils, and such soils also contain few agglutinates. Finally, the ilmenite process requires that considerable material be mined, transported, and processed in order to get a reasonable amount of the desired concentrated ilmenite feedstock.

Here we propose a related process which overcomes some of the disadvantages of ilmenite reduction. We propose that oxygen can be extracted by direct reduction of native lunar pyroclastic glass using either carbon, carbon monoxide, or hydrogen. One advantage is that no concentration of ilmenite or other phases may be necessary. Some areas of the moon are thought to be completely covered by thick layers of fine volcanic ash (pyroclastic

material) from early lunar volcanos. This glass is thought to have been deposited during early fire-fountain eruptions. The famous orange glass, discovered by the Apollo 17 astronauts, Jack Schmitt and Gene Cernan, is thought to be an example of such deposits. A related version of this glass contains variable proportions of crystals and is known as the Apollo 17 black glass.

An oxygen plant which could use such volcanic ash as feedstock material without any preprocessing might be an efficient operation which would greatly reduce the need for mining and concentration compared to some other proposed processes. Another advantage of the proposed process is that mining of a uniform, fine-grained pyroclastic ash might be much easier than mining either basaltic lava flows or impact-produced regolith which usually has large rocks and even boulders scattered throughout the more fine-grained soils.

Experimental: In order to evaluate the feasibility of this proposed process we have conducted a series of new experiments on synthetic lunar glass. We exposed this powdered glass to reducing conditions (very low oxygen partial pressure in the flowing gas) in a controlled atmosphere gas mixing furnace through which various gases could be flowed, including carbon monoxide, carbon dioxide, and hydrogen. For some experiments, we also mixed the sample with carbon. The ratios of the gases could be varied to achieve the proper reducing conditions, under which oxygen bound in the samples would be extracted and combined with the gases, leaving behind the metal to which the oxygen was originally bound. The process is similar to that used by some commercial processes in the smelting of iron ore.

We conducted the experiments over a range of temperatures from 950 C at which the glass was still solid and remained as a powder to 1200 C at which the glass partially melted and behaved as a fluid. Initial glass composition (Table 1) was approximately Apollo 11 soil composition and was not too different from the Apollo 17 orange pyroclastic glass. The biggest difference between our experimental glass and the orange glass (Table 1) is that the orange glass contains more iron oxide and magnesium oxide and less silica, aluminia, and calcium oxide. Experimental conditions for the runs included reduction with carbon monoxide, reduction with elemental carbon, and reduction with hydrogen gas. After the runs, the solid samples were removed from the furnace, cooled and analyzed with Mossbauer spectroscopy to determine the relative amount of metallic iron produced.

Results and discussion: While we did not directly measure the production of oxygen from the simulated lunar glass, we measured the metallic iron produced in the sample after the run. As this metallic iron can only be produced by the extraction of oxygen from the glass, it is a direct indication of the amount of oxygen produced. Depending on the conditions of the experimental run, the oxygen extracted from the glass would combine with the added carbon to form carbon monoxide, or with the carbon monoxide/carbon dioxide flowing gas to form additional carbon dioxide, or with the hydrogen flowing gas to form water vapor. The proportion of iron in the glass which was converted to metal in the experimental runs ranged from none in the carbon monoxide runs to 11% in the 1000 C carbon run to 53% in the 1000 C hydrogen run.

The maximum conversion to metallic iron occurred for the hydrogen-reacted sample; in 24 hours, slightly more than half of the total iron was converted to metallic iron liberating its bound oxygen which presumably reacted with the hydrogen to make water vapor. The specific mechanism and kinetics of this process are not known in detail and must be the subject of additional experiments. This conversion occurs in temperature regime in which the glass is still solid and does not melt and flow. During the heating process, the glass, which initially contained no crystals, begins to crystallize and form minerals including ilmenite and pyroxene. It is not yet clear whether the metallic iron

which we observed is produced directly from the glass or whether it is produced sequentially from newly crystallized ilmenite and pyroxene, both of which contain chemically bound iron. Regardless of the exact mechanism, these results are very encouraging and imply that these new experiments may be the basis for a viable process for producing oxygen from lunar glass.

Summary and Conclusions: In synthetic lunar glass samples, Reduction of iron to a metal occurred in experiments using both elemental carbon and hydrogen as reducing agents. When carbon was used, it formed cementite (Fe_3C) in the experiments; the production of this phase in a lunar oxygen plant would be detrimental because it would tie up the carbon and prevent easy recycling of this reducing agent. While additional steps might be developed to decompose the cementite and recover the carbon, this would add to the complexity of the process and likely significantly increase the mass and cost of the required systems. No measurable reduction occurred when the carbon monoxide/carbon dioxide mixture was used. Reduction with hydrogen was by far the most effective of the three processes.

These preliminary experiments suggest that reaction of lunar composition glass with hydrogen may be a viable process which should be considered for further technology development. The details of the mechanism are yet to be determined. If this process behaves similarly with Apollo 17 pyroclastic orange glass composition, (Table 1) and were 50% efficient at reducing the iron to metal (as demonstrated in our experiments for the 24 hour run), it would produce 24.5 kg of oxygen for each metric ton of lunar pyroclastic glass mined and processed. For comparison, a similar amount of unconcentrated high-titanium typical mature lunar soil contains only about 2% free ilmenite grains which, if concentrated and extracted with hydrogen at 100% efficiency,would yield about 2 kg of oxygen per metric ton of mined soil. If all of the ilmenite were concentrated by a magnetic or electrostatic process before chemical processing, the yield would go up to about 100 kg of oxygen per metric ton of processed ilmenite, but 50 tons of soil would have to be mined to provide the ilmenite. It seems clear that the reduction of lunar pyroclastic glass may have some advantages over lunar ilmenite reduction and should be studied in greater detail.

A practical, efficient, working process to produce oxygen on the moon would be an extremely valuable technology in the context of possible future lunar operations. Someday a small plant on the surface of the moon may be set up to process nearby volcanic pyroclastic ash deposits and produce tanks of liquid oxygen which can serve as propellant for rockets shuttling back and forth from the site and can also provide life support for the occupants of the lunar outpost.

Table 1. Composition of synthetic starting material and comparison with lunar materials

	Synthetic lunar glass	Apollo 11 soil 10084	Apollo 17 orange glass
SiO_2	44.65%	41.0%	38.57%
TiO_2	6.59	7.3	8.81
Al_2O_3	13.42	12.8	6.32
Cr_2O_3	0.14	0.31	0.75
Fe_2O_3	0.00	0.0	0.0
FeO	13.95	16.2	22.04
MnO	0.14	0.22	0.30
MgO	7.38	9.2	14.44
CaO	12.25	12.4	7.68
Na_2O	0.50	0.38	0.36
K_2O	0.02	0.15	0.09
P_2O5	0.02		0.04
Total	99.06%	99.96%	99.40%

WANTED:

LUNAR DETECTIVES TO UNRAVEL THE MYSTERIES OF THE MOON!

CRIME TO BE SOLVED:

"MASS EXTINCTIONS" ON THE MOON BY METEORITE IMPACT!

Clive R. Neal, Dept. of Earth Sciences, University of Notre Dame, Notre Dame, IN 46556; and **Lawrence A. Taylor**, Dept. of Geological Sciences, University of Tennessee, Knoxville, TN 37996.

EXECUTIVE SUMMARY - Since the return of the first lunar rocks by Apollo 11 astronauts, lunar detectives (scientists) have been attempting to unravel the "crimes" that have affected and created the Moon as we see it today. And the Earth's sister planet is revealing facts about its ancestry which is common both to the Moon and Earth. You see, the Moon's thermal and dynamic nature ended some 3,000,000,000 (3 *billion*) years ago and what we see with the Mare fillings (i.e., the dark "eyes of the Man in the Moon") is the final death throw of the Moon as a living planet. Since then, the Moon has remained effectively dead. Largely because of the lack of an atmosphere and abundant water, the Moon has remained relatively unchanged for the past 3 *billion* years. In contrast, the Earth had a similar early history, starting with its birth some 4.6 *billion* years ago, but has remained in a lively state throughout its history. In fact, the ancient ancestry of the Earth has been largely obliterated by more recent activity, such as plate tectonics, on this frisky and very much alive (and kicking) planet. Therefore, by studying the rocks and soils which make up the "death-mask" of the Moon, we are gaining insight into the early evolution of our own planet Earth.

The only weathering and erosional agent on the Moon is meteorite and micrometeorite bombardment. Due to the lack of water-induced chemical weathering, the composition of the Moon rocks has remained largely unaltered since formation. Or have they?? Meteorites have smashed, melted, metamorphosed, and otherwise affected the lunar rocks. Which rocks are unadulterated?? This is where the "lunar detective" comes in. In order to determine the "*pristinity*" of lunar rocks, we use some of the same logic and chemistry that has permitted us to determine a correlation between Mass Extinctions of life on Earth, such as the Dinosaurs, and giant meteorite impacts. We look for a chemical evidence or signature of meteorite contamination in the element **IRIDIUM**. As on Earth, the lunar rocks contain scarcely any iridium. Therefore, when anomalous iridium contents are observed, the sample has obviously been contaminated by meteoritic matter and the results from our study of the origins of such rocks can be quite misleading.

Therefore, the lunar geologist must not only be a detective in unravelling the mysteries of the Moon, but also judge, jury, and chief executioner in deciding whether or not certain returned samples are *pristine* for analysis. This paper outlines the criteria and clues we look for in identifying contamination as we continue our quest for more knowledge regarding the evolution of the Moon and the early Earth.

PRISTINITY - Warren and Wasson [1] presented 7 criteria for establishing the pristine nature of highland rocks: 1) low elemental abundances of nickel, iridium, and gold - these "siderophile" elements are abundant in meteorites, so the levels in lunar rocks must be very low relative to these meteorites (i.e., $<3 \times 10^{-4}$ x meteorite abundances); 2) low "incompatible" element abundances, i.e., elements which do not like to "fit in" to most mineral structures - these abundances are measured relative to the incompatible-element-rich lunar component "KREEP" ($< 5 \times 10^{-3}$ x KREEP); 3) coarse grains (> 3mm); 4) antiquity (> 4.2 Ga); 5) homogeneous mineral composition; 6) low $^{87}Sr/^{86}Sr$ (< 0.6992) - this ratio is changed by radioactive decay of Rb to Sr at a constant rate and can yield a time constraint in constructing a model for the formation of the rock; 7) "cumulate" character (i.e., the texture appears as if the minerals have settled or cumulated from a liquid). However, Warren and Wasson [1] originally and in their subsequent publications, have intertwined criteria for establishing *pristinity* with those for establishing a

monomict nature (i.e., is the sample comprised of only one rock type?). It is obvious that if a sample is non-pristine, it contains two components - lunar and meteoritic - and cannot be *monomict*. However, a sample can be pristine, in that no meteoritic component is present, but two (or more) lunar lithologies may be present, so this sample is again *polymict* (the sample is comprised of more than one rock type). Warren and Wasson [1-4] indicate that it is the level of "siderophile" elements present in a lunar sample which holds the key to demonstrating pristinity. This was also emphasized by Anders [5] who stated that lunar samples containing > 0.1 parts per billion Iridium are non-pristine.

Iron/Nickel Metals - Metallic fragments are ubiquitous in both lunar rocks and meteorites. Criteria must be established to distinguish between lunar and meteoritic metals. Ryder et al. [8] used Iron/Nickel metal compositions to define pristine and non-pristine highland lunar rocks. Generally, pristine rocks contain Iron/Nickel metals with a Nickel/Cobalt ratio of generally < 5, with the Mg-Suite of highland rocks proving the exception. However, non-pristine samples would be expected to contain Iron/Nickel metals with Nickel/Cobalt ratios of < 5, as well as > 10, as they are mixtures of meteoritic and pristine lunar metal. Goldstein and Yakowitz [9] attempted to define a range of meteoritic Iron/Nickel metal Nickel/Cobalt ratios which could be used to identify meteoritic contamination. However, this field was based upon *whole-rock* Nickel-Cobalt contents of *iron meteorites*, not the Iron/Nickel metal of *chondritic meteorites*, which are considered to form the bulk of the meteorite contamination on the Moon. In fact, the petrography of the metallic phases can also be useful in identifying a meteoritic component. The presence of the mineral *schreibesite* as well as *cohenite* is indicative of meteorite contamination [10], as the formation of carbon-bearing minerals in lunar rocks cannot occur without some meteoritic input [11]. Also, if *kamacite* and *taenite* inclusions are present in Iron/Nickel metal, this requires much slower cooling rates than is normal for lunar igneous rocks (e.g., 10-100° per m.y.) - which can only be achieved within the larger meteorite parent body [12-14]. The shape of the Iron/Nickel metal grains can also give clues to the pristinity of a lunar sample. If large (i.e., > 0.2mm), the grains are usually inherited from the projectile - chemical analysis of the metal is often used in conjunction with this observation [15].

MONOMICT NATURE - Criteria used to define whether one or more lunar lithologies have been mixed in during meteorite impact are less well defined. These rocks may be pristine with regard to meteorite contamination, but still *polymict* (see above). The initial criterion is that of texture. If a sample is of widely varying grain size ("brecciated") or granular, the sample is more likely to be polymict. However, as was the case of Apollo 14 sample 14310, meteorite-induced impact melting of existing rocks can produce "monomict" textures upon cooling. The key to understanding 14310 was the "straw-like" and "cross-hatched" nature of the mineral feldspar [16,17]. This texture is produced by melting to just below or, very briefly, above the absolute melting point of the lunar material. Another textural criterion in defining impact melts and rocks affected by impacts is the presence of many minute, interstitial metal grains distributed in cracks. This is indicative of "auto-reduction" (caused by hydrogen implanted from the sun by solar-wind) of a lunar rock or soil upon meteorite impact and may not contain any meteoritic contamination. This may not necessarily indicate the mixing of several components, but denotes brecciation and other criteria should be applied to make sure of a monomict nature. Warren and Wasson [1-4] stated that homogeneity between mineral grains of the same species is indicative of pristinity. We agree with Warren and Wasson [1] that such homogeneity is indicative of a monomict nature in lunar rocks formed below the surface (i.e., "deep-seated") of the Moon. However, Lindstrom and Lindstrom [18] noted that rocks from Apollo 16 exhibiting clearly polymict textures, had essentially re-equilibrated to almost homogeneous mineral compositions. Also, this criterion is not applicable to lunar rocks extruded and cooled at the surface of the Moon, where phase inhomogeneity is the rule rather than the exception. Also, for deep-seated rocks, attempting to recalculate the whole-rock composition from analyzed mineral compositions can be used to test for a monomict sample. If the whole-rock composition cannot be reproduced, this suggests another component has been included in the whole-rock sample which is not observed in the sample used to make the determinations of mineral chemistry. However, this must be used in

conjunction with texture and mineral homogeneity in order to be definitive - the whole-rock composition could be reconstructed from the mineral chemistry of a polymict rock if all components are present in both the samples used to determine whole-rock and mineral compositions.

Many lunar breccias have "KREEPy" incompatible element abundances and ratios (see above) and are polymict rocks. This suggests that KREEP forms an important constituent of lunar soils (e.g., [19,20]). Therefore, if a lunar sample contains high "incompatible" element abundances, other criteria outlined above must be used to establish a monomict nature. Warren and Wasson [1-4] stated that plutonic rocks containing incompatible elements > 5×10^{-3} x KREEP were not pristine - this criterion is used here to mean monomict as meteorites would not elevate the incompatible elements to these "KREEPy" levels (remember that KREEP is an incompatible-element-rich lunar component). This may be true for some deep-seated samples, but cannot be used as a generalization because the presence of incompatible-element-rich minor phases (e.g., [21]) rather than from mechanical mixing. Hence this criterion must be used in conjunction with others to establish the polymict/monomict nature of a given lunar sample. Furthermore, Salpas et al. [22] described Apollo 17 breccia 72275 as containing clasts compositionally indistinguishable from the breccia matrix. This breccia was derived from one or a series of closely related KREEP basalt flows, as were the included clasts. There is very little contamination of this breccia by meteorite or other lunar lithology, and as such, this breccia may be considered pristine and monomict!

LUNAR GLASSES - So far, this discussion has centered upon rock samples. However, the lunar glass beads have also produced significant petrogenetic advances in our understanding of the Moon (e.g., [23,24]). The problems involved in distinguishing pristine, primary glass beads from meteorite-induced impact melts and non-pristine glasses is slightly different. Pristine, volcanic glasses must be of basaltic composition, possess within-sample homogeneity, contain no bubbles, have a surficial coating of volatile material, and high Magnesium/Aluminium ratios, but contain no exotic inclusions. Stone et al. [25] used a type of "magnetic resonance" analysis to determine the volcanic or impact origin of glass beads. This criterion was presented in terms of I_S and glass beads containing high values of I_S are consistent with an impact origin. This is in response to the solar-wind induced auto-reduction of metallic Fe in the lunar soil upon meteorite impact. Therefore, glass beads of volcanic origin possess low I_S values. Furthermore, only those glasses with CaO/Al_2O_3 (calcium oxide/aluminium oxide) ratios of greater than 0.75 are considered to have mare parentage. Those with CaO/Al_2O_3 ratios < 0.75 are considered to be of highland parentage and formed by meteorite impact. Delano [24] concluded that in a lunar magma, Nickel will act as a lithophile element and form a positive correlation with MgO. If glass beads have been "doped" with Nickel from meteorite impact, they will form horizontal extensions from this positive correlation on a Nickel (parts per million) vs. MgO (magnesium oxide) (wt%) plot.

DISCUSSION - The above criteria have been outlined in order to demonstrate the complexity of determining whether or not a lunar sample is pristine and monomict. It is evident that *a sample may be pristine, yet may not be monomict*. Also, a sample may be **texturally** monomict, yet non-pristine. After a review of the literature (e.g., [1-8]), it is apparent that confusion can occur when authors use the terms monomict and pristine synominously. Warren and Wasson [1-4] used terms of "possibly" or "probably pristine" to describe some highland samples because either the data were lacking or there were conflicting results from the various criteria used to define pristinity. We suggest that the study of all lunar samples should first define, using the criteria summarized above, if a sample is pristine (i.e., free of meteorite contamination). Then criteria pertaining to a monomict/polymict sample should be applied. The ideal situation is that we have pristine, monomict samples, but this is not always the case. However, from our studies of Apollo 14 and 17 highland samples [25,26], we propose that pristinity is not the most essential criterion to be met in the study of lunar samples. More important is whether or not more than one ***lunar*** lithology is represented in our sample.

Although a lunar rock is non-pristine, and by definition polymict (i.e., it contains components from 2 or more sources), it may only contain **one** *lunar* rock type. If this is the case, which can be generally satisfied by applying the above criteria for defining monomict/polymict samples, then such samples may be used in the interpretation of lunar evolution in that particular area. This is because a measure of the meteorite contamination can be guaged from Iridium and Gold abundances, and even in soils, this is generally < 1%. As it is envisaged that many meteoritic projectiles would have vaporized upon impact, this addition was probably due to infiltration of meteoritic material in the vapor phase. Such a mechanism may account for the small amount of meteoritic contamination found in many lunar rocks. Addition of such a small proportion of meteoritic material by whatever means, will have practically no effect on the incompatible trace element abundances or ratios - only the inclusion of other lunar components will radically alter these. Adherence of small amounts of tough matrix to clasts during breccia pull-aparts, such as with Apollo 17 samples [26], will indicate a non-pristine, polymict sample, when in fact the clast in monomict and pristine.

CONCLUSIONS - Pristinity should not be the primary consideration in the study of lunar rocks. The most important criterion to establish is whether or not the lunar sample contains more than one ***lunar*** rock type. Even if a sample is non-pristine, as long as only one lunar rock type is present, petrogenetic interpretation can still be carried out.

REFERENCES: **[1]** Warren & Wasson (1977) PLPSC 8th, 2215; **[2]** Warren & Wasson (1978) PLPSC 9th, 185; **[3]** Warren & Wasson (1979) PLPSC 10th, 583; **[4]** Warren & Wasson (1980) Proc. Conf. Lunar Highlands Crust, 81; **[5]** Anders (1978) PLPSC 9th, 161; **[6]** Norman & Ryder (1979) PLPSC 10th, 531; **[7]** Palme (1980) PLPSC 11th, 481; **[8]** Ryder et al. (1980) PLPSC 11th, 471; **[9]** Goldstein & Yakowitz (1971) PLSC 2nd, 171; **[10]** El Goresy et al. (1972) PLSC 3rd, 333; **[11]** Gooley et al. (1973) PLSC 4th, 799; **[12]** Axon & Goldstein (1972) EPSL 16, 439; **[13]** Axon & Goldstein (1973) EPSL 18, 173; **[14]** Hewins & Goldstein (1975) LS VI, 356; **[15]** Misra & Taylor (1975) PLSC 6th, 615; **[16]** Lofgren (1974) Am. J. Sci. 274, 243; **[17]** Nabelek et al. (1978) PLPSC 9th, 725; **[18]** Lindstrom & Lindstrom (1986) PLPSC 16th, in JGR 91, D263; **[19]** Meyer et al. (1971) PLSC 2nd, 393; **[20]** Warren (1988) Apollo 14 Workshop; **[21]** Neal & Taylor (1989) GCA 53, 529; **[22]** Salpas et al. (1987) PLPSC 17th, in JGR 92, E340; **[23]** Delano & Livi (1981) GCA 45, 2137; **[24]** Delano (1986) PLPSC 16th, in JGR 91, D201; **[25]** Stone et al. (1982) PLPSC 13th, in JGR 87, A182; **[26]** Neal et al. (this volume); **[27]** Eckert et al. (this volume).

MAGELLAN: PRELIMINARY DESCRIPTION OF VENUS SURFACE GEOLOGIC UNITS.

R. S. Saunders[1], R. Arvidson[2], J. W. Head III[3], G. G. Schaber[4], S. C. Solomon[5], E. R. Stofan[1], A. T. Basilevsky[6], J. E. Guest[7], G. E. McGill[8], and H. J. Moore[4]
[1]Jet Propulsion Laboratory, [2] Washington University, St. Louis, [3] Brown University, [4] United States Geological Survey, [5] Massachusetts Institute of Technology, [6] Vernadsky Institute, USSR, [7] Univ. London Observatory, [8] Univ. Massachusetts

This preliminary report summarizes geologic observations from approximately one-half of the Magellan nominal eight-month mission to map Venus. Preliminary compilation of initial geologic observations of the planet reveals a surface dominated by plains that are characterized by extensive and intensive volcanism and tectonic deformation. We have identified four broad categories of units- Plains Units, Linear Belts, Surficial Units and Terrain Units.

PLAINS: The surface of Venus is dominated by plains; 80% of the surface lies within 0.5 km of the mean planetary radius[1]. Four types of plains have been classified in the Magellan data analyzed to date. Plains may have discernible flow units, and may be characterized by small domical hills. The data reveal a far more complex surface of the plains than previous data. (1) **Smooth plains**- planar, areally extensive units characterized by a featureless appearance with no discernible flow units and few domical hills or linear features. These plains are interpreted to be emplaced by volcanic flooding where the flows have homogenized with time or by coalescing shield emplacement with shields of too low slope to be detected in high incidence angle radar images. (2) **Reticulate plains**- planar, areally extensive units characterized by one or more sets of sinuous, radar-bright lineaments unresolvable as ridges or grooves. An example can be seen in Guinevere Planitia where the reticulate plains are embayed by younger radar-dark flows. Linear features within the reticulate plains tend to be spaced > 5 km apart. Reticulate plains are interpreted to be flood or shield-type plains, that embay underlying structure and/or have been subjected to later deformation. 3) **Lobate plains**- planar regions characterized by radar-bright and/or radar-dark lobate regions that extend for 10's to 100's of kilometers. The type example of Lobate plains is seen at Mylitta Fluctus. The plains tend to be topographically controlled. Lobate plains have few or no linear features; if present, fractures tend to control emplacement of plains materials. Lobate plains are interpreted to be volcanic in origin, representing coalescing flows and flow complexes. (4) **Grid Plains**- planar, areally extensive regions characterized by intersecting orthogonal sets of radar-bright lineaments. The example located in Guinevere Planitia, extends for hundreds of kilometers with very regular spacing. Linear features within the Grid Plains lack sinuosity of linears seen in Reticulate Plains, and tend to be spaced closer (<5 km). These plains are interpreted to have been affected by complex tectonic deformation.

LINEAR BELTS: Two types of linear belts have been identified- ridge belts and groove belts. These units were also identified in Venera 15/16 data of the northern hemisphere of Venus, with the largest number of belts located in the Atalanta Planitia region[2]. The units are identified based on the predominant form of tectonic feature and the topography. (1) **Ridge belts**- belts of linear structures predominated by ridges. A large grouping of ridge belts is found in Lavinia Planitia,. Ridges tend to lie in linear belts of increased radar brightness interpreted to be increased roughness due to mechanical erosion. Belts tend to extend for 100's of kilometers, and have topographic relief of 1 km or less. Ridges within the belts tend to be spaced 5-20 km apart. Ridge belts are interpreted to be compressional in origin, sometimes cut by later episodes of extensional deformation. (2) **Groove Belts**- belts of linear structures predominated by grooves or troughs. Several groove belts are seen in Lavinia Planitia, with grooves spaced 5-20 km apart. The groove belts generally have greater topographic relief than the ridge belts. The grooves are interpreted to be extensional in origin.

SURFICIAL UNITS: Magellan has revealed a number of material units not previously identified in previous data sets, with the exception of the crater materials unit. Six material units have been

identified. (1) **Crater materials**- radar-bright deposits located within and surrounding craters. Material surrounding the craters generally has lobate boundaries and a hummocky appearance. Crater materials units are interpreted to be of impact origin. (2) **Channel materials**- generally sinuous, radar-dark, 1-3 km across materials located in both plains and highland regions. A channel located in Guinevere Planitia is a few kilometers across, and extends for over 500 km. The channel materials are interpreted to be basaltic lava. In some cases channels are carved into the older surface and are analogous to Lunar sinuous rilles. (3) **Bright Lobate surficial material**- radar-bright to mottled materials contiguous with crater materials, characterized by lobate boundaries. The deposits may extend for 100s of km and may be 10s of km wide, and may surround small shields or domes of probable volcanic origin. Emplacement of material tends to be topographically controlled, and boundaries of the unit tend to have increased brightness. Bright Lobate Surficial Material units are interpreted to be outflow of highly fluid material, probably volcanic in origin, caused by the cratering process. (4) **Bright material**- Relatively radar-bright materials that tend to have linear or feathered appearance. Bright material frequently appears contiguous with ridges or small domical hills, or appears as long (> 100 km) linear units. Bright material is interpreted to be areas of increased roughness of the surface due to deposition of removal of material by the wind. (5) **Dark material**- relatively radar-dark materials that have a circular diffuse appearance or appear as long (> 100 km) linear units. Dark material is interpreted to be areas of increased smoothness due to deposition of material. (6) **Linear faceted material**- linear occurrences of relatively radar-bright facets. The material occurs in groups of lineations, typically extending for < 100 km. This unit may represent sand dunes.

TERRAIN UNITS: A number of terrain units have been identified in Magellan data. Two of them, Groove and Ridge Terrain and Cross-lineated Terrain, are in regions previously identified as tessera[3]. The units here follow more typical unit divisions based on morphology, and may be thought of as morphologic subdivisions of larger, more complex geomorphologic regions called tessera. (1) **Groove and Ridge Terrain**- relatively raised (< 1 km) units characterized by intersecting sets of grooves and ridges. Groove and ridge terrain tends to occur in small patches, surrounded by smooth or reticulate plains, as seen in fragments of this terrain on Lakshmi Planum. Grooves and ridges tend to be spaced less than 10 km apart. Regions of Groove and Ridge Terrain tend to be relatively radar-bright and approximately equidimensional. This unit is usually part or all of a region of tessera, and is interpreted to be highly deformed basement unit that has been subsequently embayed. (2) **Cross-lineated Terrain**- relatively high (< 1 km), areally extensive, equidimensional terrain characterized by intersecting sets of lineaments generally unresolvable as ridges or grooves. The lineaments are spaced approximately 10 km apart, and are in some cases identifiable as graben. This unit has formed by complex deformation. (3) **Mountainous Terrain**- high (highest elevations > 1 km above surrounding region) terrains characterized by long (> 100 km) linear ridges and valleys frequently cut by shorter grooves and ridges. Mountainous terrain sometimes has either a belt-like or a more equidimensional appearance, and tends to be radar-bright. Mountain belts form the borders of Lakshmi Planum. The mountains are interpreted to form from compressional deformation, followed by relaxation and extension.

The Venusian surface appears to be geologically young yet quite geologically active. Highlands show geomorphologically diverse appearances, possibly indicating multiple origins and modes of evolution for highland terrain on Venus. This classification is preliminary, and will evolve as we see more of Venus. The Soviet Venera 15/16 data and the geologic analysis [3] has provided invaluable guidance in planning and carrying out our preliminary analysis.

ACKNOWLEDGEMENTS: This work was carried out, in part, by the Jet Propulsion Laboratory, California Institute of Technology, under NASA contract.

REFERENCES: [1] Masursky, H. et al.,**JGR, 85**, 8232, 1980, [2] Barsukov, V.L. et al.,**Proc. LPSC 16th**, in **JGR**, 91, B4, D378-398, 1986, [3] Sukhanov, A.L. et al., **USGS Map I-2059**, 1989.

EFFECTS OF A GIANT IMPACT ON URANUS.

W. L. Slattery, Los Alamos National Laboratory, and W. Benz and A. G. W. Cameron, Harvard-Smithsonian Center for Astrophysics. (Press version)

Tilt of Uranus Axis. What is often regarded as one of the most distinguishing and unique properties of the Uranus system is the fact that its rotational axis is tilted 97 degrees to the plane of the ecliptic (the plane in which the planets rotate around the Sun). The planet rotates with a period of 17.24 hours, and this rotation is thus actually in a retrograde direction.

However, from the point of view of the origin of the Uranus system, what counts is not that the rotation is actually retrograde, but rather that the tilt of the axis is not close to zero. If a planet is assembled from a very large number of small objects, then its rotation is expected to be prograde and the angle of inclination small. For example, Jupiter and Saturn are mostly composed of hydrogen and helium, which are expected to have been collected into the planet as gases, and indeed their tilts are small and their rotations are prograde. In the case of Uranus, only about 15 per cent of the mass is hydrogen and helium, and the remaining material, primarily water, ammonia, hydrocarbons, rock, and iron, can all be collected into the planet in solid form. This means that much of this material can have been assembled into bodies of intermediate size before colliding with Uranus. With only a very small number of these bodies in the mass range around 10 per cent of the Uranus mass, the angular momentum brought in when the largest of these collides with Uranus can become a large part of the final angular momentum now possessed by the planet. When this largest planetesimal collides, the direction of the collision is essentially random. Thus the final direction of the spin axis of the planet will also be essentially random.

When we wish to do a numerical simulation of this largest planetesimal collision, the actual angle of the collision plane is not meaningful; what is meaningful is the value of the angular momentum transferred to the growing planet. We choose to measure this in terms of the rotation period that the planet acquires following the collision, having started at the beginning of the collision with no rotation at all. We shall take as a measure of a successful simulation of a Giant Impact on the planet that the rotation period should become 17.24 hours or less. It is obvious that this criterion can only be regarded as an approximate one, since the final rotation rate will depend to some degree upon the collisions with the next largest group of planetesimals.

The Satellites of Uranus. Uranus has a compact system of regular satellites lying in the plane of its equator; these revolve around the planet in the same direction as its rotation, so that they are retrograde satellites.

Such a system of regular satellites will tend to line up their orbital planes to match the equatorial plane of the planet. If the planet were slowly, over something like a million year time period, to tilt its rotation axis relative to the plane of the ecliptic, then the plane of the satellite orbits would follow. However, if the rotation axis were suddenly tilted, as in a major collision, there would be no time for the orbital planes of the satellites to tilt with it. If the tilt were more than 90 degrees, then the orbital planes of the satellites would still be attracted to the equatorial plane, but in this case the satellites would revolve in a direction opposite to the rotation of the planet. For the orientation that Uranus now has, these would become prograde satellites. If the large tilt of the Uranus axis were produced by a Giant Impact, a pre-existing set of regular satellites could not tilt their orbital planes to match the new axis.

This gives rise to the hypothesis that the existing set of regular satellites might have

been produced as a consequence of the Giant Impact itself. These satellites have mean densities 1.4 times that of water, about what you would get with a solar mix of ices (i. e., water, ammonia, and hydrocarbons), rock, and iron. In any event, it is clear that it is not sufficient for the Giant Impact just to deposit the ices in orbit; rock and iron must also be placed in orbit either from the Giant Impact itself or due to trapping of infalling solid materials in the equatorial plane by the ices left there by the Giant Impact. This question makes it particularly interesting to determine those Giant Impact parameters that leave rock and iron in orbit in addition to ices.

The Calculations. The simulations of possible Giant Impacts were carried out using Cray supercomputers at Los Alamos. The technique used is called smooth particle hydrodynamics (SPH). In this technique the material in the proto-Uranus planet and in the Impactor is divided into a large number of particles which can overlap one another so that local averages over these particles determine density and pressure in the problem, and the particles themselves have their own temperatures and internal energies. During the course of the simulation these particles move around under the influence of the forces acting upon them: gravity and pressure gradients. This is the technique that we have used to study collisions involving large bodies in the terrestrial planet region, particularly in connection with the problems of the origin of the Moon and of the high mean density of Mercury.

There are a number of uncertainties involved in the construction of models of the proto-Uranus and the Impactor that reflect our uncertainties about the manner in which these bodies were formed. We do not know when the Giant Impact might have occurred, but we think it would have been early in the life of the solar system, late in the general planetary accumulation process. For this reason we can use present-day models of Uranus only as a general guide, since the precollision Uranus was probably hotter than now, and it may have been more thoroughly mixed, with rock and iron dissolved in a convective atmosphere. However, we have followed conventional planetary structures by giving both the proto-Uranus and the Impactor an iron core surrounded by a rock (dunite) mantle. The Impactor was given an atmosphere composed of the ices H_2O, NH_3, and CH_4 in relative solar proportions. The atmosphere of the proto-Uranus was composed of these ices with an additional 2 $M_\oplus$ of hydrogen and helium mixed into them.

Simulations of possible Giant Impacts were made with the SPH code. We used 5000 particles in the proto-Uranus and 3000 particles in the Impactor. The physical properties of the materials used in the models are provided by their equations of state, which we obtained from a variety of sources.

Many numerical simulation runs were made, varying the mass of the Impactor between 1 and 3 $M_\oplus$ (but keeping the sum of the Impactor and proto-Uranus masses equal to that of Uranus today), and varying the angular momentum in the collision. The velocity of the Impactor at infinity in all the simulations was set at 5 km/sec.

A summary of all the simulations is shown in the figure. A horizontal line is drawn at the present value of the Uranus rotational period, 17.24 hours. The angular momenta on the abscissa are in units of 10^{43} gm cm^2/sec. The large range in collisional angular momenta corresponds to a small range of planetary rotational periods because part of the Impactor can sometimes escape from the system following the collision. A low angular momentum collision leads to core impact and absorption of the Impactor. Higher values of the angular momentum will lead to an atmospheric passage which slows down the Impactor, which then rises to a height of several planetary radii, with its core tidally sheared and separated from the atmosphere, to be followed by an infall that absorbs most of the Impactor core in the core of proto-Uranus.

GIANT IMPACTS ON URANUS Slattery, W. L. *et al.*

Most of the collisions leave ice in orbit. The energy released by the impact heats the proto-Uranus so much that the ice in orbit will be in gaseous form in the temperature field of the atmospheric radiating surface. Some of the collisions also leave some rock in orbit. These collisions are shown by filled symbols in the figure.

None of the simulations with an Impactor mass of 1 $M_\oplus$ leaves Uranus rotating with a period as short as the present-day value, although some of them come close; this Impactor mass can therefore be stated as a lower limit to the probable Impactor mass needed. An Impactor mass of 3 $M_\oplus$ succeeds over a wide range of collisional angular momenta in producing a Uranus rotation period shorter than at present, which we regard as acceptable, but in none of the cases is rock left in orbit. This is not necessarily fatal for the satellites, because an orbiting disk may capture significant amounts of rock-containing planetesimals that impact upon it; we are almost completely ignorant of the satellite accumulation conditions. However, for all Impactor masses in the range 1.3–2 $M_\oplus$ there were collisions which both spun the planet fast enough and left rock and ice in orbit.

Thus the simulations have not selected a narrow range of Giant Impact conditions that would be needed to produce the observed Uranus system, but have proved to be quite permissive. We believe that the high temperature and mixing results of the collisions will be of interest to those trying to model the history of the system.

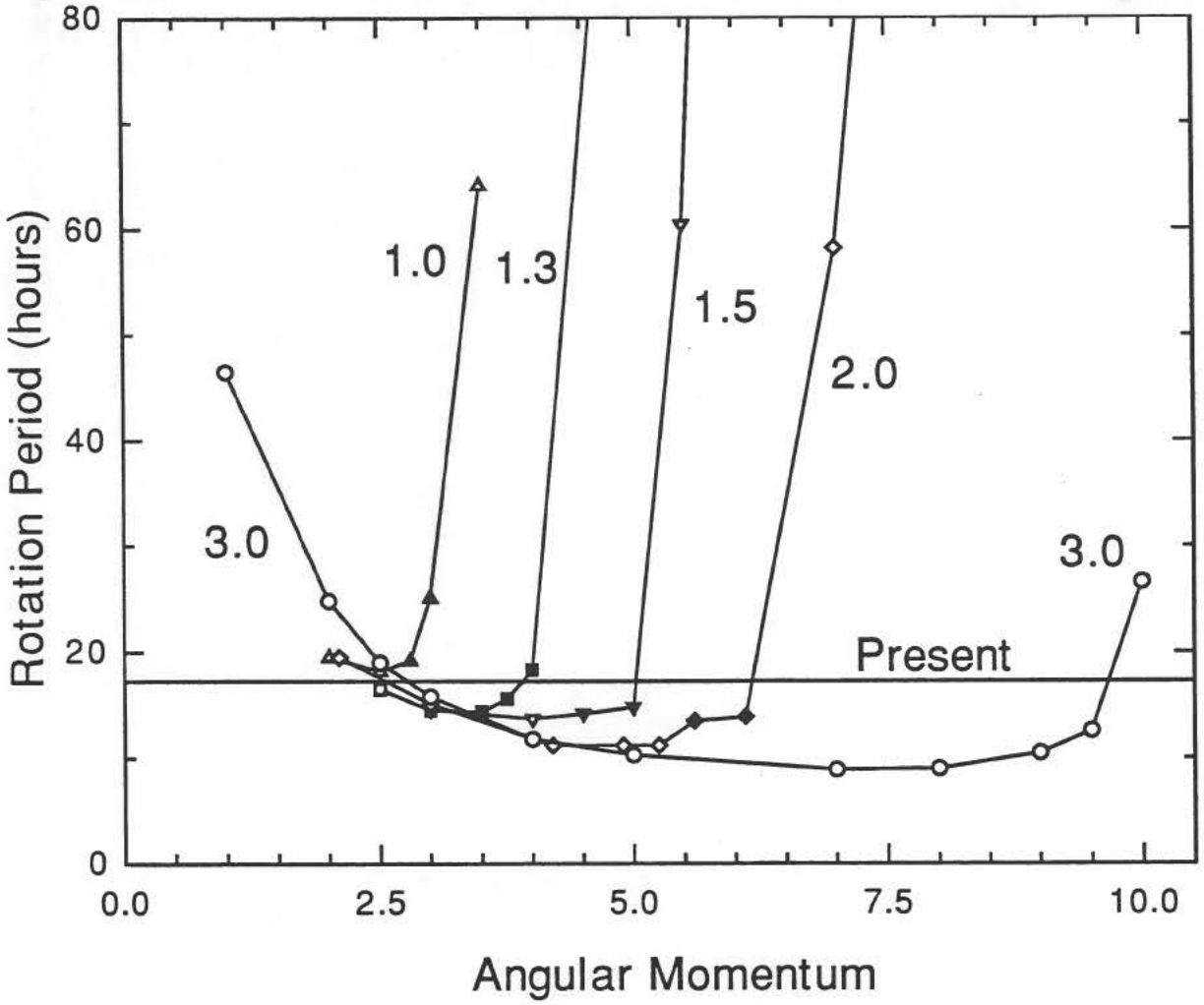

COSMIC DUST - LABORATORY ANALYSES OF EXTREMELY SMALL PARTICLES

Frank J. Stadermann, McDonnell Center for the Space Sciences and Physics Department, Washington University, St. Louis, Missouri 63130, USA.

In order to learn something about the origin, the history, and the composition of our solar system, there are a number of different approaches that can be used. One can make theoretical calculations, computer simulations, astronomical observations, active and passive space craft experiments. A different approach involves the laboratory analyses of extraterrestrial material. The results of such measurements may give some information on the history and origin of that individual extraterrestrial sample. This information can then be added to the overall picture we have of our solar system. Unfortunately there are only few classes of extraterrestrial material available for laboratory research. Among them are lunar samples from the Apollo missions and meteorites, which have been an object of scientific research for a long time already. Compared to meteoritics, the laboratory study of cosmic dust particles has long been neglected. However, this was not due to little interest in this class of extraterrestrial material, but was a consequence of the enormous experimental difficulties in the analyses of 10 micron size dust particles. Only when advances in the field of micro analysis made it possible to gain meaningful results from a few nanograms of sample material, more effort was focused on cosmic dust particles.

Where do these cosmic dust particles come from and how are they collected? Most of the extraterrestrial dust particles in the vicinity of the Earth are probably produced in the asteroid belt or stem from comets. These particles then form a dust cloud that covers the entire inner part of our solar system. By its gravitational force the Earth attracts several tons of these dust particles every day, which then decelerate on atmospheric entry. Although some particles burn up, others survive atmospheric entry and can then be collected for laboratory analyses. Currently cosmic dust particles are routinely collected at a number of different sites, like, e.g, Antarctica, Greenland, and the stratosphere. The major advantage of collecting particles in the stratosphere is the fact that these dust particles have not been exposed to weathering as much as cosmic dust particles collected on the surface. The dust collection in the stratosphere is done by NASA, using high-flying aircraft at a height of 20 kilometers. All measurements reported here were made on these stratospheric dust particles.

Cosmic dust particles are sometimes also called 'micrometeorites', which may be a somewhat misleading term, since it seems to imply that these dust particles are basically meteorites, only smaller. Although many properties of cosmic dust particles are still unknown, one thing can be said for sure: These particles do not fit straight away into the standard classification scheme that has been developed for the 'classical' meteorites. This means that cosmic dust particles really represent their own class of extraterrestrial material, that is distinctly different from everything else that is available for laboratory research. This is exactly the reason why so

much effort is put on the analyses of these tiny particles. Hopes are that we might learn something from these dust particles, that we could not learn from other classes of extraterrestrial material.

Most problems arising in the experimental work with cosmic dust particles can generally be attributed to one of two major difficulties: contamination and size. Contamination with terrestrial dust particles is a problem, since even in clean environments, such as the stratosphere, more than 50 % of all captured dust particles may be of terrestrial origin. It is therefore necessary to identify cosmic particles before meaningful results can be obtained. There are no easily-recognizable distiguishing marks of a cosmic dust particle; in fact, cosmic dust looks very much like terrestrial dust. An indication for a cosmic origin is, e.g., an anomalous isotopic composition. In theory this identification has to be done for each dust particle individually, but in most cases this is impractical and an identification depending on second-order characteristics is prefered. However, this procedure may lead to incorrect assumptions on whether an individual dust particle is of cosmic or terrestrial origin.
Size-related problems are for the most part obvious. Many analytical measurement techniques can not at all be used for the analysis of dust-size particles. And some other techniques may require so much material, that analyses are restricted to one single measurement per particle. This is especially disadvantageous, since it turned out that cosmic dust particles are a heterogeneous class of extraterrestrial material. Therefore it is desirable to use analytical techniques that make a number of complementary measurements on the same particle possible.

All measurements on stratospheric dust particles presented here were made with secondary ion mass spectrometry SIMS , which is a destructive technique, i.e., the sample is "used up" during the course of measurements. However, the amount of sample material used for each individual measurement is so small, that several different analyses can be made with each individual dust particle. The SIMS technique turns out to be an extremely useful tool in the study of very small particles and in the work presented here it made a number of "firsts" possible: The nitrogen isotopic compositions of cosmic dust particles have been measured for the first time. It was also the first time that it was possible to measure the abundances of the Rare Earth elements in these particles. However, the most important advance this work represents is the fact, that both trace elemental and isotopic abundances have been sucessfully measured in the same particles. Thus it is, for the first time, possible to compare isotopic and trace element abundance data of the same cosmic dust particles.

Significant hydrogen and nitrogen isotopic anomalies have been found in several cosmic dust particles. These anomalous isotopic compositions probably originated in cold interstellar molecular clouds that predate the solar system. Material from these interstellar clouds must later have been incorporated in these dust particles or their parent body, which were able to retain some kind of isotopic memory to those early stages. When the oxygen isotopes were measured, most cosmic dust particles turned out to have normal,

i.e. terrestrial, compositions. Only in one particle a clearly different, anomalous oxygen isotopic composition has been observed, that strongly resembled the oxygen measured in refractory inclusion in chondritic meteorites. At least this one particle might have a direct relationship with some meteoritic inclusions. In order to investigate this further, it was very helpful that the trace elemental abundances were also measured in the same particles.
Trace elemental abundances of extraterrestrial material can be compared with "cosmic abundances", i.e., average solar system abundances. When a sample contains all trace elements at cosmic abundances then it is assumed that the sample consists of unaltered, "primitive" material. Most of the analyzed cosmic dust particles have compositions that identify them as such primitive material. However, there is one notable exception; the particle with the oxygen isotopic anomaly has very different trace element abundances, which are similar to those found in refractory meteoritic inclusions. It looks like this one cosmic dust particle has an interesting story to tell. A small amount of material from this particle is still left and will be used for mineralogical analyses.

Although cosmic dust particles are extremely small samples of extraterrestrial material, they contain a great deal of information about the conditions at the time when they were formed and about their history. The real problem is not that these samples are too small, but that many measurement techniques are still not sensitive enough. Every advance in the field of micro analyses will most likely broaden our knowledge about these particles' real origins. Thus, every piece of information gathered in the laboratory can contribute to the overall picture we have of our solar system.

WHAT WERE THE EFFECTS OF THE FORMATION OF THE BOREALIS BASIN, MARS?; **Kenneth L. Tanaka**, U.S. Geological Survey, Flagstaff, Ariz. 86001

Why study Mars' Borealis basin?

Borealis basin, in the northern hemisphere of Mars, is a vast, subcircular, lowland region that constitutes a third of the planet's surface area. The basin is several kilometers lower in elevation than much of the highland regions that characterize the remainder of the planet. The rim of the basin is seen to be intensely eroded and fractured where it is not buried by young deposits. Although Borealis is large and has been studied by many workers, the nature of its origin and its possible influence on climate and subsequent geologic structures have remained elusive problems. Some workers have thought that it formed by single or multiple impacts of asteroid-size bodies. Other workers have favored a tectonic origin, whereby the basin records a major geologic event in which the crust was lowered by overturn of material deep within the planet. Moreover, the basin provides Mars' largest sink for sedimentary materials deposited by wind and water, and it may also have contained ancient lakes or even an ocean. If large bodies of water once existed in the basin, they may have deposited thick carbonate layers that formed at the expense of carbon dioxide in the atmosphere. This atmospheric change would have reduced air temperature and pressure. Open bodies of water would have no longer been stable, and permafrost would have become more deeply entrenched in the Martian crust.

What progress has been made in the study of the Borealis basin?

The impact theories for the origin of the basin require its formation during intense bombardment (in the Early Noachian Epoch) to explain the lack of ejecta deposits and the paucity of possible ring structures observed along the Borealis rim. However, recent geologic mapping and crater-density studies, which form the basis for determining the relative ages of Martian surfaces and features, show that major erosional and structural features along the rim of the basin are Late Noachian to Early Hesperian in age. Thus the features formed after the early intense meteorite bombardment of the planet. If the features formed because of basin formation, an impact origin is ruled out. A tectonic origin, on the other hand, is compatible with a later time of formation. George McGill and Andrew Dimitriou of the University of

Massachusetts noted that volcanism over the planet peaked during the Late Noachian/Early Hesperian; they proposed that this coincidence with the timing of basin formation can be explained by a major tectonic event of global proportions.

My results complement these recent studies and conclusions. I suggest that erosional features along the basin rim formed from ground-water runoff that was initiated by tectonic lowering of the basin. The lowering caused ground water to flow from highland rocks into the basin. The variety of the resulting erosional features is astounding--they include channels of various sizes, morphologies, and tributary patterns; intensely eroded terrains made up of scattered hills and mesas; collapse features such as chaotic terrain, floor-fractured craters, pits, and troughs; and flood plains. The channels are widely accepted as having formed by runoff and sapping processes, and the eroded terrains may also have been subjected to the same processes as well as to secondary mass-wasting. The collapse features are suggestive of erosion or compaction of subsurface material, perhaps due to liquefaction and ground-water flow. These interpretations require that large tracts of highland rocks be made up of loose, fine debris that is easily eroded and transported and capable of trapping and releasing large volumes of water. Also, a few discontinuous troughs formed by collapse are found exclusively in northern latitudes (> 30° N.), where permafrost may have been deep when the troughs formed. The troughs may have been produced by tunnel erosion caused by ground-water rivers that once flowed below impermeable frozen ground.

The discharges of ground water required to produce these erosional features would have been extremely large. Although evidence for comparable discharges is not found on Earth, many similar discharges (chiefly related to tectonic events) are recorded on Mars in later time periods, and one of these discharges is similar in magnitude. No evidence of large-scale flooding prior to formation of the Borealis basin is found on the surface of Mars.

How did runoff of ground water into the Borealis basin affect Mars' climate?

Researchers are still uncertain about early atmospheric conditions on Mars. Thus the following suggestions are highly speculative.

If the early atmosphere was much richer in carbon dioxide than the present atmosphere, as many workers think, then atmospheric temperatures and pressures may

BOREALIS BASIN, MARS: Tanaka K.L.

have been higher. These conditions could have permitted the stability of large lakes or even a small ocean in the Borealis basin (particularly at lower latitudes). In turn, the open water would have facilitated relatively rapid carbonate formation. Atmospheric carbon dioxide would have been reduced, eliminating the earlier greenhouse conditions. As these changes took place, much of the equatorial surface and near-surface water would have been transferred to the polar caps. The colder temperatures would cause the permafrost zone to deepen. As a possible result, the depth of that zone today probably exceeds one kilometer all over Mars.

*U.S.GOVERNMENT PRINTING OFFICE:1991-561-057/20102

ANTARCTIC METEORITE EET87521 IS A BASALT FROM THE MOON; G.F. Herzog, Dept. Chemistry Rutgers Univ., New Brunswick, NJ 08903; M.M. Lindstrom, NASA Johnson Space Center, Houston, TX 77058.

Background - A special session at the 22nd Lunar and Planetary Science Conference will be devoted to a discussion of a meteorite named EET87521 that came from the Moon. Most kinds of meteorites come from the asteroid belt. Lunar meteorites are most likely produced by the impact of asteroidal or perhaps cometary matter on the Moon and are especially interesting because 1) they represent parts of the Moon from which we have no other samples and 2) they tell us something about the process by which rocks travel from the Moon to the Earth.

Although EET87521 was not the first lunar meteorite, all seven studied before it had come from the lunar highlands, the areas on the Moon that appear bright to the naked eye. Unlike the other lunar meteorites, EET87521 is mostly a dark-colored basalt, similar to those that make up the lunar mare or seas, which formed when enormous pools of molten rock cooled and crystallized.

Basaltic lunar meteorites such as EET87521 were unknown until a little over a year ago when the lunar origin of this meteorite was discovered by Delaney [1] and Warren and Kallemeyn [2]. In the past year three additional basaltic lunar meteorites have been found in the Japanese Antarctic meteorite collection. These four basaltic meteorites all appear to be distinct individuals. There are seven known meteorites from the lunar highlands, but they appear to represent at most four distinct meteorites. This 50-50 distribution of highland-mare lunar meteorites contrasts strongly with the 83-17 distribution of highland-mare areas observed from photogeology. Either the statistics of lunar meteorites are grossly unrepresentative or some mare basalts are hidden in what appears to be highland regions.

New Results - Four papers in the session at the conference deal with the chemical and mineral composition of EET87521. Delaney et al. [3] and Takeda et al. [4] describe the mineralogy and petrology of EET87521. The rock consists of little pieces of mare basalt welded together with smaller grains of basalt and glass. J. Delaney of Rutgers Univ. describes the petrography and composition of several basalt fragments that have a range of mineral compositions suggestive of differentiation.

Dreibus et al. [5] and Lindstrom et al. [6] discuss the major and trace element composition of several samples selected from EET87521. Both show that there is significant compositional variation from location to location in the meteorite. Although some of this variation is due to addition of small amounts of highland materials, M. Lindstrom (Johnson Space Center) argues that magmatic differentiation is responsible for the major differences between samples. This small meteorite may contain the remnants of a series of related lava flows.

Three papers [7-9] reconstruct the path that EET87521 traveled in order to get to Earth. All the authors agree that this meteorite took as little or less time than any other lunar meteorite to make the trip, under 150,000 years, and perhaps only days or weeks. In contrast, most meteorites from the asteroid belt are in transit for millions of years.

The very short transit times for EET87521 and other lunar meteorites surprised some scientists who study the impact process. They had originally thought that most of the material launched from the Moon would have enough energy to escape not only from the Moon's gravitational field but from the Earth's as well. Once out of the Earth's field, however, it was shown that a lunar meteorite would take a very long time to be re-captured. Based on the new evidence of short transit times, it now seems likely that lunar meteorites can have relatively low speeds when blasted off the Moon.

ANTARCTIC LUNAR METEORITE EET87521; G.F. Herzog and M.M. Lindstrom.

How much material does the Moon send to Earth? We know that at least 8 samples from the Moon with masses ranging from an ounce to a pound were produced and traveled to a small area in the Antarctic within the last million years. There is no reason to expect more or fewer lunar meteorites to land in the Antarctic than anywhere else. Accordingly, an average, world-wide arrival rate of about 1 million lunar meteorites/million years is indicated. Most of these meteorites would fall in the oceans and be lost. Those that fall on continents in temperate climates would be weathered away fairly quickly. But the continental US should have been struck by thousands of lunar meteorites in the last million years and we might expect some of them to have survived.

References

1) Delaney J.S. (1989) Lunar basalt breccia identified among Antarctic meteorites. *Nature* **342**, 889-890.

2) Warren P.H. and Kallemeyn G.W. (1989) Elephant Moraine 87521: the first lunar meteorite composed of predominantly mare material. *Geochim. Cosmochim. Acta* **53**, 3323-3330.

3) Delaney J.S., Warren P.H., Kallemeyn G.W. and Hervig R.L. (1991) Petrography of samples for consortium studies of the Elephant Moraine 87521 very-low titanium lunar breccia. *Lunar Planet. Sci.* **XXII**.

4) Takeda H., Mori H. and Miyamoto M. (1991) Mineralogical studies of lunar mare meteorites EET87521 and Y793274. *Lunar Planet. Sci.* **XXII**.

5) Dreibus G., Palme H., Spettel B. and Wänke H. (1991) The lunar meteorite Elephant Moraine 87521: a mixture of low Ti mare basalt and highland material?

6) Lindstrom M.M., Martinez R.R. and Lipschutz M.E. (1991) Evidence for magmatic differentiation in matrix lithologies of basaltic lunar meteorite EET87521. *Lunar Planet. Sci.* **XXII**.

7) Eugster O., Michel Th. and Niedermann S. (1991) Regolith history of lunar meteorites EET87521 and Yamato-793274. *Lunar Planet. Sci.* **XXII**.

8) Nishiizumi K., Arnold J.R., Sharma P., Kubik P.W., Klein J. and Middleton R. (1991) Cosmic ray exposure history of lunar meteorite EET87521. *Lunar Planet. Sci.* **XXII**.

9) Vogt S., Herzog G.F., Klein J. and Middleton R. (1991) Exposure history of the lunar mare basalt EETA 87521. *Lunar Planet. Sci.* **XXII**.